UNIVERSITÄT BAYREUTH

Characteristics of Arctic methane emission via chamber measurements

Master's thesis

by

Marcus Wildner
Student number: 1288290

in fulfilment of the requirements for the degree of Master of Science

Geoecology - Environmental Science: Micrometeorology and Atmospheric Chemistry
Faculty of Biology, Chemistry and Earth Science
University of Bayreuth, Germany

February 18, 2015

Supervisor:

1. Prof. Dr. Thomas Foken
Department of Micrometeorology
Faculty of Biology, Chemistry and Earth Science
University of Bayreuth, Germany

2. Prof. Dr. Andreas Held
Department of Atmospheric Chemistry
Faculty of Biology, Chemistry and Earth Science
University of Bayreuth, Germany

Contents

Abbreviations

ALD	Active layer depth
BVOC	Biogenic volatile organic compounds
C	Carbon
Ch	Chamber
CRDS	Cavity ringdown spectroscopy
DOC	Dissolved organic carbon
EC	Eddy covariance
ER	Ecosystem respiration
GWP	Global warming potential
LGR	Los Gatos Research
NEE	Net ecosystem exchange
OA-ICOS	Off-axis integrated cavity output spectroscopy
OH	Hydroxyl radical
PAR	Photosynthetic active radiation
pH	Degree of acidity (-log[c_{H^+}])
RE	Radiative efficiency
RF	Radiative forcing
SD	Standard deviation
UGGA	Ultra-portable greenhouse gas analyser
WS-CRDS	Wavelength-scanned cavity ringdown spectroscopy

Symbols

A	Area	cm^2
p	Pressure	hPa
R	Ideal gas constant	hPa K^{-1} mol $^{-1}$
sl	Slope	ppm s^{-1}
T	Temperature	°C
V	Volume	cm^3
M	unreactive molecule	
M_C	Molar mass of carbon	g mol^{-1}
σ	wavelength precision	MHz

List of Figures

List of Tables

Abstract

The understanding of methane emission from Arctic peatland soils presents a key role for climate development in present and future, since these thawing peatlands store large amounts of carbon in the soil. This thesis investigated therefore CH_4-emissions in the permafrost region of north-east Siberia. Complementary to micrometeorological methods non-automatic, non-steady-state flow-through chambers were configured with different setups for a cumulative flux detection of CH_4 and CO_2. Different fan, inlet tube and air path designs inside the chambers have been tested under laboratory and field conditions, to develop improved flux detection methods for greenhouse gases. Even the bias of changed fluxes through large shaped tussock plants as an obstacle thereby could be obviated. Particularly in field conditions fluxes stabilised if fans and integrated inlet tube system were used to create an horizontal air stream inside a closed chamber. However, fluxes were influenced by flooding situation, vegetation, atmospheric conditions such as air pressure and air temperature as well as soil conditions, e.g. soil temperature and active layer depth. In this study the emission pathways of methane were determined, with regard to ebullition. Frequencies of ebullition events occurred in mid of July and beginning August, while the proportion of ebullition on total fluxes increased steadily until August and reached on average 2 to 7 % during the summer season. Mainly episodic events were detected with carbon amounts of 2 to 1100 mgC m^{-2} d^{-1}. Coherences of ebullition was found with increased total CH_4-flux as well as with environmental conditions. These results are used for series of studies, which further more deeply focus on passive plant-mediated transport of CH_4 and the combination of chamber data with micrometeorological data of wavelet analyses and conditional sampling.

Zusammenfassung

Im Verständnis um die derzeitige Klimaentwicklung nimmt die Methanemission aus arktischen Mooren eine Schlüsselstellung ein, da die zunehmend abtauenden Dauerfrostböden enorme Mengen an Kohlenstoff speichern. Daher fanden die hier vorliegenden Experimente über CH_4-Emissionen in Nordost-Sibirien statt. Ergänzend zu den mikrometeorologischen Methoden wurden dabei nicht-automatische, kumulierende Durchflusskammern verwendet und mit verschiedenen Konfigurationen für die Untersuchung eines linear ansteigenden CH_4- und CO_2-Flusses getestet. Dazu wurden Ventilatoren zur Belüftung, Einlassluftsysteme und Luftzirkulation innerhalb der Kammern unter Labor- und Feldbedingungen untersucht, um die Treibhausgasemission künftig besser bestimmen zu können. Selbst voluminöse Tussocks mit möglichem Einfluss auf die Luftzirkulation beeinflussten durch die angewendeten Konfigurationen kaum noch die Gasemissionen. Vor allem unter Feldbedingungen halfen Ventilatoren und ein integrierendes Einlassluftsystem um die Flüsse zu stabilisieren, indem ein horizontaler Luftstrom in einer geschlossenen Kammer erzeugt wurde. Allerdings beeinflussten Vegetation, atmosphärische Bedingungen wie Luftdruck und Lufttemperatur, aber auch Bodentemperatur und Auftautiefen solche Gasflüsse speziell in gefluteten Böden. Außerdem wurden in dieser Arbeit Methanemissionspfade untersucht, besonders im Hinblick auf Ebullition. Häufig traten diese Ereignisse Mitte Juli und zu Augustbeginn auf, wohingegen der Ebullitionsanteil am Gesamtfluss bis August stetig zunahm und durchschnittlich 2 bis 7 % erreichte. Hauptsächlich episodische Ereignisse traten als Ebullitionen auf mit Kohlenstoffmengen von 2 bis 1100 mgC m^{-2} d^{-1}. Zusammenhänge von Ebullition mit ansteigenden CH_4-Gesamtflüssen, atmosphärischen Einflüssen und Bodenbedingungen wurden festgestellt. Diese Ergebnisse sind Teil einer Untersuchungsreihe mit weiteren Schwerpunkten auf CH_4-Emissionen über indirekten Pflanzentransport und der Kombination von Kammermessungen mit mikrometeorologischen Methoden wie Waveletanalyse und Conditional Sampling.

1 Introduction

1.1 Motivation

Climate change is dependent on greenhouse gases, such as CO_2 and CH_4 (Ciais et al., 2013), which play a major role in the process of global warming. If the climate shows variations, e.g. in surface air temperature, precipitation and wind, which persist several decades, the climate situation is about to change (IPCC, 2013). Therein the impact of anthropogenic and natural influences have to be determined (Bridgham et al., 2013), considering the involved biogeochemical cycles (subchapter 1.2) and feedbacks (subchapter 2.2). With respect to the carbon cycle this consideration includes the greenhouse gases CO_2 and CH_4 with the highest global warming potential (GWP) in the atmosphere (Myhre et al., 2013). The release of carbon is observed from wetlands, contributing 10 - 40 % to the GWP (Bridgham et al., 2013). Thus, the dynamics of global stocks of carbon compounds have to be understood. In the northern hemisphere frozen soils store a large proportion of organic carbon that is expected to be released throughout climate change (Zimov et al., 1997). Increased thawing of these permanent frozen soils in the Arctic will lead to a positive feedback cycle and more greenhouse gases will be released (Ciais et al., 2013). Measuring methods (subchapter 2.4) and more data on methane fluxes are necessary for a better prediction of these processes and improving these methods will help to achieve that (McGuire et al., 2009). Especially methane shows a different pattern of fluxes from soils to the atmosphere at flooded areas than at dry areas (Bridgham et al., 2013). These circumstances require an adequate adjustment of measuring compared to usual determination methods of climate changing gases (subchapter 2.4.2). Present CH_4-emissions at wetlands of ca. 164 Tg per year (Bridgham et al., 2013) could rise up to 600 Tg per year until 2100 (Gedney et al., 2004).

1.2 Methane in Arctic wetland soils

The enhanced greenhouse effect by CH_4 compared to CO_2 in the stratosphere causes a positive feedback (Ciais et al., 2013). This effect spreads to the lower troposphere and leads to surface temperature rising in summer times. In winter from October to May (Merbold et al., 2009) snow and ice inhibit the gas exchange between soil and atmosphere. Nevertheless, even in wintry permafrost with generally warmer conditions CO_2 and CH_4 also can be produced by decomposition, release after snow melt and active layer thawing. This process results from the formations of non-frozen parts between active layer and continuous zone, so called taliks (Windsor et al., 1992; O'Connor et al., 2010).
The release of bound CO_2 due to permafrost thawing and spreading of the active layer in summer leads to the metabolisation of released carbon and modern fixed CO_2 to CH_4 by

microorganisms in anoxic zones (Ciais et al., 2013) of standing water on plane soils. In a concrete case study of Klapstein et al. (2014) the modern fixed carbon showed 7 % of released carbon and 90 % of modern fixed CO_2. Methane emerges from fermentation (Conrad, 1996) of organic matter under anoxic conditions by methanogenic microorganisms (Whalen, 2005):

$$CO_2 + 4\,H_2 \longrightarrow CH_4 + 2\,H_2O \tag{R1}$$

Organic carbon as an electron donor is metabolised by heterotrophic microbes and drives decomposition (Bridgham et al., 2013). Especially root exudates and carbon out of former CO_2-sequestration via photosynthesis promote the metabolisation to CH_4 via acetate. Another path of metabolisation in anaerobic, saturated zones (catotelm) poses the fermentation of polymers via degradation by microbial exoenzymes to monomers, fatty acids and alcohols either to acetate or to H_2 and CO_2 by fermenting bacteria and afterwards to CH_4 (Bridgham et al., 2013). Moreover, parallel to the CH_4-production also CO_2-production out of fatty acids and alcohols occur due to electron acceptance via alternative terminal electron acceptors: (1) denitrification: $NO_3^- \longrightarrow NH_4^+$, N_2; (2) manganese reduction: Mn (III, IV) $\longrightarrow$ Mn (II); (3) iron reduction: Fe (III) $\longrightarrow$ Fe (II); (4) humic reduction; and (5) sulphate reduction: $SO_4^{2-} \longrightarrow S^{2-}$, S^0. In consequence, the reaction R1 is part of a cycle that also leads to nitrogen emission with N_2, N_2O and NO into the atmosphere via denitrification (Conrad, 1996). Since the CO_2 : CH_4 production ratio seems too small if it is only explained with fermentation and methanogenesis, other processes, e.g. fermentation byproducts, low pH and particularly phenolic / aromatic substances, have to contribute to more CO_2-proportion as well (Bridgham et al., 2013). Additionally, the deeper the thawing depth the more CO_2 will be converted into CH_4 in water saturated zones by methanogenesis (O'Connor et al., 2010). Consequently, relevant amounts of CH_4 only affect the climate if enough water is available for the reduction of CO_2, while avoiding CH_4-oxidisation.

There are three main pathways for methane emission from permafrost soils (Whalen, 2005): (1) direct diffusion of generated methane between soil particles via soil water and soil air, (2) delayed ebullition events due to bubbling as a form of mass transport (subchapter 2.4.3), (3) passive plant-mediated transport through plant tissue via diffusion.

Gas emission through ebullition has been considered less in the past for which reason it is investigated in this thesis. Ebullition can have a significant effect on CH_4 as its hydrophobic properties allow the formation and release of bubbles to the unsaturated soil pore space or directly to the atmosphere, if CH_4 is produced in sufficiently high concentrations (O'Connor et al., 2010). Despite, ebullition is less determined (Bridgham et al., 2013) and its controlling processes are largely unknown. Although permafrost is normally less permeable for gases from deeply occurring hydrates its permeability increases up to five orders of magnitude by

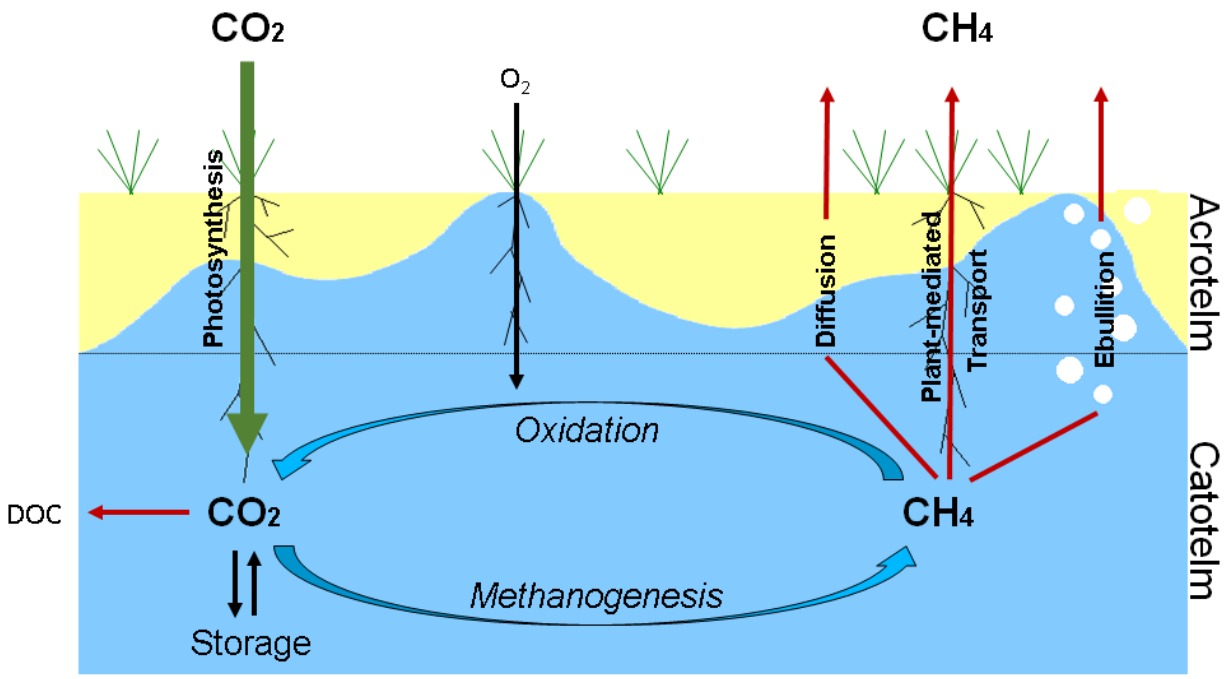

Figure 1: CH_4-circle in Arctic wetland soils (in parts from Whalen, 2005; Iturraspe, 2010). Production and consumption are blue arrowed, incoming carbon is green arrowed, outgoing carbon is red arrowed. Water saturation in acrotelm varies with the ground water level, catotelm is always flooded.

warming as temperature rise to 0°C (McGuire et al., 2009). Yet it is largely unknown how ebullition exactly occurs and if it essentially contributes to CH_4-emissions in permafrost soils under terrestrial conditions (Klapstein et al., 2014).

Apart from a methanogenic emission of methane from anoxic soils there is also a biotic contribution to the atmospheric CH_4-concentration via plant transmissions, so called plant-mediated transports. Such plants have aerenchyma, which are able to conduct gases from the soil to the atmosphere and vice versa (Kutzbach et al., 2004). Especially plants adapted to wetlands or aquatic conditions show this ability, originally used to transport oxygen from the shoots to the roots. This pathway works in flooded areas with soil respirations as a fast and low-resistant possibility for CH_4 without being re-oxidised to CO_2 (O'Connor et al., 2010). Atmospheric CH_4-concentrations do certainly not rise above soil CH_4-concentrations under flooded conditions in the presence of gas conducting plants. Therefore, the gas conduction of aerenchyma can be considered as a one-way transport for methane due to diffusion effects and second law of thermodynamics. Frequently occurring species with aerenchyma in Arctic regions are cotton grass (*Eriophorum angustifolium*) and aquatic plants, adapted to temporarily, partly or fully flooded ecosystems with a certain water level that allows plants to reach both soil and air (Figure 1). Despite its release in wetlands, 40 - 70 % of CH_4 is re-consumed by methanotrophic bacteria in aerated soils (Megonigal et al., 2005), aerobic

soil zones and the rhizosphere (Whalen, 2005; Fritz et al., 2011). Consequently, methane once produced can be oxidised under aerobic conditions in unsaturated soils (acrotelm), e.g. due to oxygen transported through the aerenchyma of plants (Whalen, 2005):

$$CH_4 \longrightarrow CH_4OH \longrightarrow HCHO \longrightarrow HCOOH \longrightarrow CO_2 \qquad \text{(R2)}$$

1.3 Scientific questions on methane emission

In this study a closed dynamic chamber system was used to detect reliable gas fluxes of CH_4 and CO_2 on a small scale; more precisely the methane emission pathway of ebullition from the soil to the atmosphere in northern permafrost peatland and its dependence on environmental conditions. The later collaboration with eddy-covariance, wavelet analyses and conditional sampling presented in the work of Schaller (2015) will follow afterwards. For the methodical setup it is important to know if ventilation through fans is necessary for a measured flux that is closer to the natural fluxes. In case it is the constellation of the installed fans have to be investigated (Davidson et al., 2002). Measurements with and without fans during a single flux recording may show a direct relation to ventilation and a stable flux. The influence of environmental conditions like incoming radiation, air temperature or air pressure to the flux should be determined as well (Xu et al., 2006), since a closed measuring system alter the natural gas fluxes. Therefore, sensitivity studies are necessary to assess the influence of different chamber setups on the measured fluxes (subchapter 2.4.2).
Hitherto, the spontaneous bubbling of methane is poorly understood particularly in terms of terrestrial ebullition (subchapter 2.4.3). Mostly coincidental events were detected in short term recordings and are hard to predict (Rosenberry et al., 2003). A more systematic analysis ensues with longer and specific measurements on ebullition. Further, more data on CH_4-emission is needed especially on ebullition events (Ciais et al., 2013) and CH_4-release via ebullition events will be more important in the future due to higher estimated temperatures and therewith permafrost thawing. CH_4-release is triggered by changes in water level, air pressure decline (Tokida et al., 2005), temperature changes, spring thaw of ice and mechanical disturbance (Coulthard et al., 2009; Couwenberg, 2009). While other studies (Rosenberry et al., 2003; Glaser et al., 2004) focused on the bubble formation through soil level rise and fall, in this study the length, frequency, absolute amount and relative proportion of ebullition events to the total methane emissions are extracted. Additionally, the appearance depending on environmental conditions and the frequency during the summer season are interesting facts for the evaluation of ebullition (Windsor et al., 1992) and is studied in this work. The ebullition frequency is expected to increase with higher temperatures and water level due to improved methanogenesis activity and Windsor et al. (1992) also saw more events with

dropping water levels caused by the release of stored methane in soil pores.
Beside the still unknown amount of CH_4-emission caused by temperature increases the influence of wetland plants has to be explored (O'Connor et al., 2010; Ciais et al., 2013). Therefore, plant-mediated transport will be determined further in related studies of Kwon (2015). This study focused on methodical possibilities improving chamber measurements of methane out-gassing from soil to atmosphere. Secondarily the detection of ebullition is being investigated.

2 Theoretical background

2.1 Arctic carbon in greenhouse gases

The majority of carbon is stored in oceans, soils (organic matter and peat) and vegetation (Zimov et al., 2006). Soils gain carbon by CO_2-uptake through photosynthesis and loosing carbon by leaching of dissolved organic carbon (DOC) into rivers and by emissions of CO_2 and CH_4 (Figure 1). The atmosphere above the Arctic is influenced by CH_4-sources, which introduce 3 - 9 % of net land produced CH_4 (15 - 50 Tg) per year (McGuire et al., 2009) that gets lost to the atmosphere by mostly seasonally unfrozen wetlands (Ciais et al., 2013). This amount constitutes currently about 10 % of global wetland loss and in future could rise up to 3.5 x 10^5 Tg of CO_2-equivalents (that are similar to other biogeochemical feedbacks) and thereof 5000 Tg CH_4, excluding the effect by lakes. Due to thawing of permafrost more carbon in compounds of CO_2 and CH_4 will be released and would act as greenhouse gases, which warm up the atmosphere by absorbing solar radiation and thereby promotes a positive feedback (Klapstein et al., 2014). Higher radiative forcing (RF) causes the ecosystem to change and more primary production may cause more biogenic volatile organic compound (BVOC) releases into the atmosphere that extend CH_4-lifetime, if wet conditions for CH_4 production are available (O'Connor et al., 2010). Additionally, microbial heat release forces higher biotic soil activity, e.g. decomposition rates and leads to permafrost thawing as well, even though the frozen soil layer with a thickness up to several hundred metres in continuous zone (Figure 2) has a relatively long sustaining time before thawing (O'Connor et al., 2010). However, the terrestrial Arctic acts as a sink to CO_2 by photosynthesis of plants. These regions probably could sequester even more CO_2 with higher temperatures because of longer growing seasons and higher vegetation productivity, even though 75 % of emitted CH_4 were fixed by photosynthesis before (King et al., 2002).

2.2 Methane cycle - properties and effects in the environment

The amount of produced CH_4 by methanogenic microorganisms is dependent on substrate availability, primary production, organic matter decomposition, soil temperature ($20 - 25°C$) and soil pH (Whalen, 2005; Couwenberg, 2009; O'Connor et al., 2010). Emission of CH_4 steadily grew in Holocene, but in 1980s this growth stagnated and CH_4-sources and -sinks came to an equilibrium until the year 2006 (Ciais et al., 2013). Several reasons for this behaviour were discussed like cleaner anthropogenic energy gain processes, less wetland and rice agricultural emissions, changes in hydroxyl radical (OH) concentrations or more stable microbial and fossil fuel emissions. Today wetlands are the biggest natural CH_4-source with emission from 177 to 284 Tg per year (Ciais et al., 2013). Boreal and Arctic tundra show

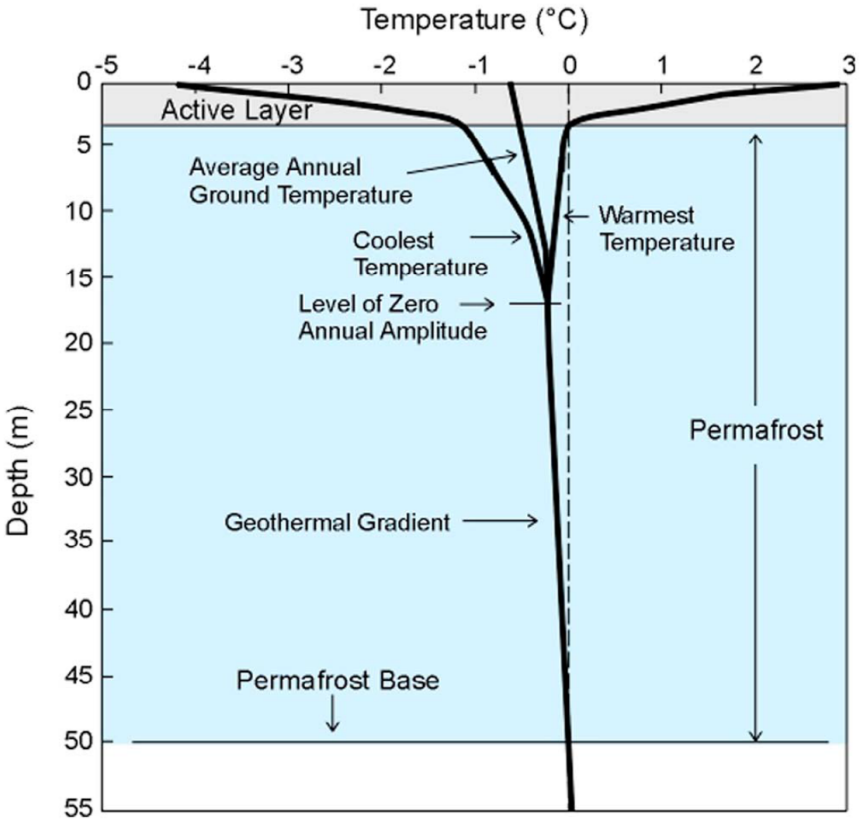

Figure 2: Permafrost illustration with different layer types and temperature dependence during the year (O'Connor et al., 2010) from: Natural Resources Canada 2010, courtesy of the Geological Survey of Canada).

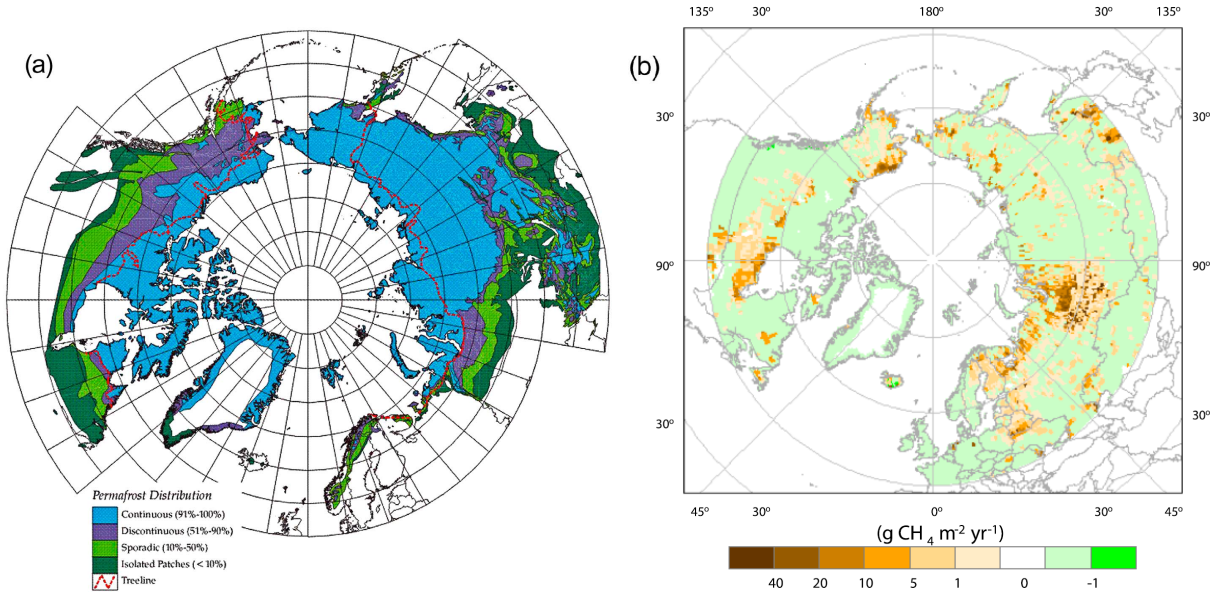

Figure 3: (a) Distribution of permafrost in northern hemisphere and (b) net CH_4-fluxes (simulated) in northern hemisphere in 1990s. Positive values: net emission, negative values: net uptake (O'Connor et al., 2010).

emission from 3.2 x 10^{-8} to 3.5 x 10^{-8} TgC m^{-2} y^{-1} on average (Whalen, 2005). It is still largely unknown how much more CH_4 is caused by temperature increases or already took place since Pleistocene before the first systematic measuring campaigns in 1930s. However, until now CH_4-emission from Siberian lakes is marginal, contributing less than 5 % to global CH_4-budget (Ciais et al., 2013). Because of long lasting responses and thawing processes of permafrost and hydrates in deep soil and ocean layers the time scale of a more important CH_4-increase may develop over millennia. Presently, stocks of methane (1.7 x 10^6 TgC) exist in permafrost (Figure 3), as frozen hydrates in ocean sediments and on the slopes of continental shelves (Schuur et al., 2008). These amounts are stable only at low temperatures and high pressures and can have far-reaching effects on climate, soil erosion and other environmental issues, especially in shallow shelve regions. However, the larger share of deeper hydrates would be oxidised while rising to water surface.

Particularly high temperatures in the Arctic and above average rainfall in the tropics in the year 2007 seemed to cause a higher increase in CH_4 (Hartmann et al., 2013). Since ice core determinations showed similar processes from boreal and tropical wetlands in the glacial past and longer lifetime in the atmosphere (Ciais et al., 2013) this effect is likely to repeat itself in future. But observations of polar CH_4-emissions showed no contributions from wetlands. Other natural sources are emissions of fossil CH_4 from geological sources like mud volcanoes, termites, oceans, marine hydrates and wild fires (Hartmann et al., 2013; Ciais et al., 2013). Anthropogenic sources for CH_4 currently are waste disposal sites, animal husbandry, energy gain, mining and leakages from extraction, biomass burning, fossil and biofuel, rice paddy agriculture and man-made lakes (Myhre et al., 2013; Ciais et al., 2013). They contribute to total CH_4-emissions with 50 - 65 %, predominantly in the northern hemisphere (Ciais et al., 2013). The economical growth of Asian countries contributes to a larger CH_4-emission growth due to their usage of coal based energy in the period from 2000 to 2008.

Currently (2011) the global mean surface concentration of CH_4 is about 1.803 ppm in dry air with an annual growth of 0.25 %, a radiative efficiency (RE) of 3.63 x 10^{-4} W m^{-2} ppb^{-1} and RF of 0.48 $\pm$ 0.05 W m^{-2} (Hartmann et al., 2013; Myhre et al., 2013). The atmospheric lifetime of CH_4 is approximately nine years (with respect to OH 11.2 $\pm$ 1.3 years or soil uptake by bacteria 120 $\pm$ 24 years and in the stratosphere 150 $\pm$ 50 years) and the often cited perturbation lifetime 12.4 $\pm$ 1.4 years. CO_2 for comparison shows global mean surface concentrations of 391 ppm with an annual growth of 0.5 %, a RE of 1.37 x 10^{-5} W m^{-2} ppb^{-1} and a RF of 1.82 $\pm$ 0.19 W m^{-2} ppb^{-1}. Although CO_2 has twice the annual growth rate the radiative efficiency of CH_4 is 26.5 times larger, even if RF of CO_2 is 3.8 times larger than CH_4, in the end, because CH_4 absorbs more infra-red radiation per molecule than CO_2 (Ciais et al., 2013). Therefore, the GWP of CH_4 in a range of 100 years is 28 (but for 20 years it is 84) compared to CO_2 as reference with a GWP of 1 (Myhre et al., 2013). Additionally,

methane reduction in the atmosphere is induced by photochemistry and reactions with OH (O'Connor et al., 2010):

$$CH_4 + OH \longrightarrow (O_2, M) \longrightarrow H_2O + CH_3O_2 \quad \text{(R3)}$$

and in smaller amounts through chemical reactions in the stratosphere (with chlorine and oxygen radicals), in marine boundary layers (with chlorine) and oxidation in aerated soils (Ciais et al., 2013). With increased atmospheric CH_4-concentrations its lifetime rises because more CH_4 reacts with OH and decreases the amount of OH such that less CH_4 can be reduced, depending on temperature conditions (O'Connor et al., 2010). Yet, OH is responsible for 90 % of CH_4-removal in the atmosphere. But by 1 % increase of CH_4 0.32 % of OH decrease in reaction (Myhre et al., 2013).

Other effects of CH_4-emissions are ozone (O_3) production and the influence on stratospheric water vapour and CO_2. Indirectly CH_4 has an increased effect on RF of other gases and on total RF with a proportion of 0.64 W m^{-2}, but it is attenuated e.g. by influences of NO_x, O_3 and ultraviolet light.

The temperature rise over the last decades already caused enhanced thawing of Arctic permafrost soils (Schuur et al., 2008). This thawing causes problems for Arctic ecosystems, e.g. release of greenhouse gases CH_4 and CO_2 or erosion of peat layers above frozen soil due to increased outflow of melt water in rivers, channels, lakes and oceans. Thereby, carbon is leached especially as DOC, former bound in ice particles (Vaughan et al., 2013). Further effects are hard to predict or model, but may lead to disturbed equilibriums in Arctic river landscapes and the north Siberian sea. However, McGuire et al. (2009) came to the conclusion that an increased CH_4 release due to erosion of coastlines and submerged permafrost cannot influence RF of the climate strongly, since the erosion mechanism is not sufficient enough to release that much CH_4 out of gas hydrate, moreover without being oxidised in thick sediment layers. Furthermore, climate feedback responses on the development of wetting or drying of landscapes, because CH_4 will be produced under wet conditions, but decreased CO_2-emissions at the same time occur due to lower decomposition rates. Additionally, it is still unclear if increased temperatures and associated permafrost thawing lead either to an increase in water level due to landscape collapse and more precipitation or rather to lower water levels due to an enhanced soil drainage (Rosenberry et al., 2006; O'Connor et al., 2010). In case of re-wetting of drained peat soils a high initial emission may be expected, but over longer periods an improved climate situation follows (Couwenberg, 2009). Contrary, Rosenberry et al. (2006) explain an ebullition decrease in peat in every case.

Arctic wetlands are likely to extend with both rise of precipitation and temperature due to thawing permafrost (Ciais et al., 2013). However, CO_2 shows an even stronger enhancement

effect on CH_4 if the climate situation is modelled. Additionally to these variable factors local influences play an important role for increased or decreased CH_4-emission like the elevation above river flooding level, drainage and runoff situation, evapotranspiration or flatness and homogeneity of landscapes, vegetation and ecosystems. Finally, changes in atmospheric chemistry, caused by fire occurrence and anthropogenic activity may influence atmospheric CH_4-concentrations as well.

2.3 Permafrost soils

Permafrost soils are enriched with carbon accumulated during the Pleistocene (McGuire et al., 2009). So called yedoma (frozen loess) soils store carbon rich organic material since the Pleistocene (Zimov et al., 2006). Permafrost is defined as frozen ground that remains below 0°C for at least two consecutive years. These soils cover 20 % of earth's terrestrial surface (Zhang et al., 1999) and generally are distinguished thermally between warm permafrost > -2°C present mostly in mountain regions and cold permafrost < -2°C found more in high latitudes (Smith et al., 2010). The seasonally iced layer above permanently frozen soils are called active layers (Figure 2), because of biologically active processes in thawing time, e.g. decomposition, root activity and organic carbon storage. Its depth indicates the effect of temperature on permafrost and their related ecosystems. Recently, temperatures of permafrost soils are rising due to higher air temperatures and altered snow coverage in the climate change situation (Vaughan et al., 2013). Tundra regions are affected by this change of conditions since they show often less soil and ice contents but more bedrock portions. Thus, temperature change is largest in high latitudes and tundra regions and lowest in places where more forested vegetation appears, since it isolates the soil. The effects of permafrost degradation especially due to temperature rises up to 2°C are observed more since 1980s, which is indicated by deeper thawing of soils in summer and expanding active layers up to 90 cm with taliks, emerging of thermokarst, development of thaw lakes and slope slides (O'Connor et al., 2010). Indirectly also the ecosystem is about to change in drier areas from tundra to taiga with higher wildfire probability due to a lower surface albedo through a higher shrub growing with longer vegetation periods as well as better soil and nutrient supply.

2.4 Chamber measurements

2.4.1 Chamber measurements versus eddy covariance

The bottom-up determination of CO_2 and CH_4 in micrometeorological fluxes (Bridgham et al., 2013) requires different techniques, which depend on local environmental factors like terrain and climate (Couwenberg, 2009). The minimisation of errors required the development of different techniques to complement each other. Eddy covariance (EC) with small towers observes gas emissions from soil in large spatial and temporal scales up to one square kilometre (Joosten and Couwenberg, 2009) and continuously over several years, respectively. This method less influences gas exchange during the measurement than chambers (Drösler, 2009) and has a higher sensitivity on fluxes controlled by atmospheric conditions. Other methods are able to screen footprints of even hundreds of square kilometres with tall towers (McGuire et al., 2009). For finer resolution in small scales from even a few millimetres in case of single plants to several metres at a plant community structure microecosystemical operations can be determined via chamber measurements, but require more effort for high measuring frequencies (Parkin et al., 2003). Topographically heterogeneous areas or certain weather situations, e.g. during night time with a stable stratification or rain fluxes are hard to detect by EC (Drösler, 2009). Besides, EC needs stationary gas concentrations over 30 minutes (Foken and Wichura, 1996), whereas ebullition detection requires higher temporal resolutions. Riederer et al. (2013) consider diurnal periods for mid-latitudes wherein EC and chamber measurements differ at morning and equalise at noon. In late afternoon chambers measure far more CO_2 than EC, which is explainable by the oasis effect with cooling situations due to negative sensible heat flux and still positive latent heat flux at the same time. Due to the observation principles of an integrated gas determination by EC detailed information in smaller scales cannot be resoluted and therefore wavelet analyses have to be considered beside chamber measurements. In contrast, chamber measurements hardly represent fluxes of an entire ecosystem (Friborg et al., 1997). Also differences between EC and chamber measurements may occur in low frequency flow patterns (Riederer et al., 2013), where EC more often underestimates gas fluxes at low turbulence intensity (Pavelka et al., 2007).

Hence, combining EC with chamber measurements may improve flux measurements (Friborg et al., 1997; Pavelka et al., 2007; Riederer et al., 2013). Both variants of determining gas emissions from soils are suitable for certain applications and a choice of methods and special devices has to be adjust for every individual case.

2.4.2 Current methodological problems with chamber setups

If the chamber is closed by the hood, no natural turbulence above the soil surface appears anymore and air pressures may change (Xu et al., 2006). During the measurement air temperature, air humidity and trace gas concentrations increase due to the missing exchange with the atmosphere (Rochette and Hutchinson, 2005). Measuring reliably and accurately fluxes poses a challenge for current chamber designs as plants have the potential to change CO_2-fluxes inside the chamber. That is why normally transparent acrylic glass for chambers is used and allows highly natural respiration and photosynthesis (Rochette and Hutchinson, 2005).

Atmospheric turbulences presently are reproduced insufficiently with chambers. To solve this problem fans are used (Christiansen et al., 2011). At this point new problems appear, e.g. incomplete air mixing or possible pressure changes inside the chamber (Xu et al., 2006). Further, different atmospheric layers can prevent long wave radiation from ascending from the soil surface. As a result merely irregularly a stable stratification forms in chambers. Overestimating CH_4-emissions by 60 - 90 % compared to EC may be the consequence (Werle and Kormann, 2001; Pavelka et al., 2007), which is e.g. caused by under pressurising the inside of the steady-state chamber (Davidson et al., 2002) or by including the first 10 - 30 sec into the flux calculation with a closed non-steady-state chamber (Christiansen et al., 2011). Underestimating CH_4-emissions can occur with small chambers (Pihlatie et al., 2013) and through saturation effects of too long closing times, with high wind speeds at night time (Christiansen et al., 2011; Riederer et al., 2013) and unmixed conditions. Others, e.g. Müller et al. (2009), used overpressurised chambers to prevent leakage and wind disturbances from the outside. Friborg et al. (1997) assumed an underestimation of flux by chambers caused by winds, as CO_2-measurements with open vented chambers (Xu et al., 2006) showed a sudden increase in flux with increased wind speeds. These wind speeds are of a similar magnitude as velocities generated by fans inside the chamber. Hence, a stable mixing condition inside the chamber is essential for accurate results, as well as for creating more natural conditions. Therefore, short closing times during the measurements with unvented chambers are preferable. The usage of direct measuring (dynamic) of enriched trace gases (closed) leads to non-steady-state flow-through chambers (Rochette et al., 1992). Using this kind of chamber Davidson et al. (2002) report an underestimation of flux by up to 15 % for small chambers, yet largest variations occur in static chambers (Pumpanen et al., 2004). For an overview of manual chambers see Figure 4. The disadvantage with non-steady-state flow-through chambers is, however, that only a few temporal windows with ebullition can be observed. Underestimation by reduced fluxes are still possible (Parkin et al., 2003) due to saturation.

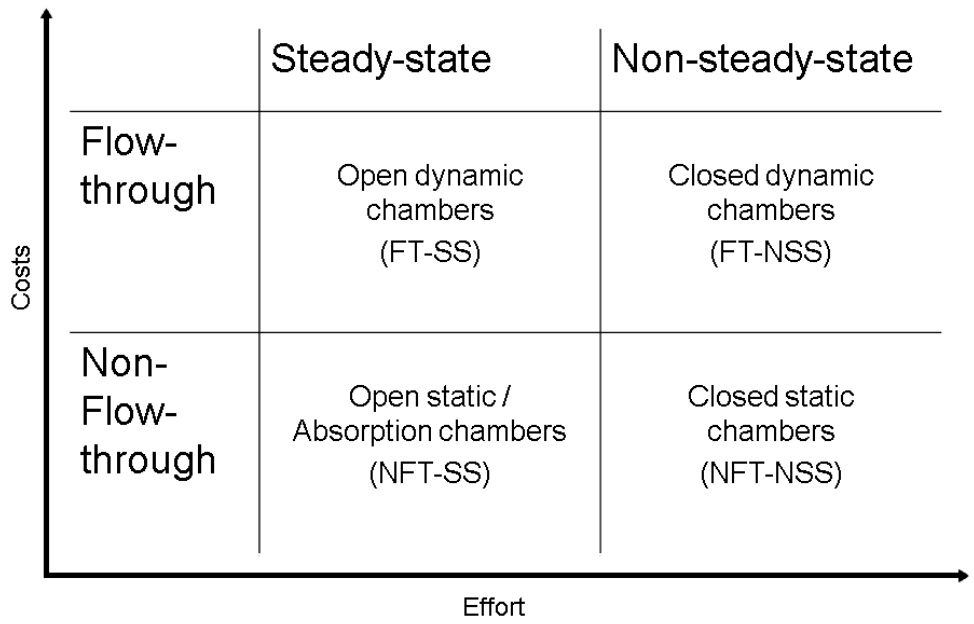

Figure 4: Manually usable chamber types (after Livingston and Hutchinson, 1995; Hutchinson and Rochette, 2003; Rochette and Hutchinson, 2005). Costs grow with dynamic in-situ-analysing of gas samples and effort grows with closing frequency and decreasing closing time.

2.4.3 Ebullition events

The production and transport of methane in the Arctic is driven by diffusion, ebullition and plant-mediated transport, which are influenced differently. This thesis investigates by which mechanisms methane ebullition events are driven and which temporal and spatial patterns occur. The influence of gas conducting plants has to be considered as well. Ebullition and plant-mediated transport have great importance to methane emission because of their ability to bypass re-oxidisation in oxic soil zones. Ebullition proportions on total methane flux range between 1 - 22 % (Martens et al., 1992; Windsor et al., 1992) in wet meadow tundra and in *Sphagnum*-dominated fens. However, they are not well determined, plant-mediated transport conducts 25 - 100 % of total emission to the atmosphere in sedge-dominated Arctic wetlands (Whalen, 2005; Bridgham et al., 2013).

In northern peatlands gas pockets consist of pores filled with methane (Glaser et al., 2004). Methane is highly hydrophobic and therefore almost insoluble in water. Hence, bubbles form easily in small soil pores, mainly in surface soil layers (Glaser et al., 2004; Klapstein et al., 2014; Yu et al., 2014), if the hydrostatic pressure by the water table and air pressure is exceeded. Especially in spring and during droughts degassings occurs in peatlands (Glaser et al., 2004). Furthermore, free gas may sustain over long periods in saturated soil zones of the catotelm and is released through a steady accumulation of bubbles contributing 20 - 45 % of soil air (Klapstein et al., 2014; Tokida et al., 2005) or 0 - 20 % of soil volume

(Rosenberry et al., 2006) before mixing with the surface atmosphere. Climate factors, such that air pressure or water table fall, cause an increase in bubble pressure in the pores. There is a distinction between ebullition into episodic events and steady-state events. Episodic events, which occur approximately 87 % of the time, form bigger bubbles out of smaller ones instead of the releasing of small bubbles throughout steady-state ebullition. The latter form of ebullition results in a spatially more homogeneous distribution (Coulthard et al., 2009; Klapstein et al., 2014), which can lead to a possible under estimation in the measurements due to reduced sensitivity at the chamber (Yu et al., 2014).
If ebullition should be linked to permafrost thawing and prospective terrestrial or aquatic hydrate release it might contribute to a rise of current atmosphere CH_4-concentrations in the Arctic (Ciais et al., 2013) by a factor of 10. Understanding the governing processes is necessary to adjust the measuring methods . Also, wind speed may influences ebullition occurrence as pressure fluctuations show similar flux patterns for CO_2 with rapidly increased wind speeds (Xu et al., 2006). The exact amount of emitted CH_4 through spontaneously occurring bubbles can not be quantified alone either with chamber measurements due to large contingency and low predictability nor with eddy covariance methods through its integration of gas concentration signals over a larger area and mixing of air until the detection (Drösler, 2009). Therefore, as for general flux detection, it is necessary to combine both techniques for the comparison of data between chamber fluxes and EC fluxes. For that task new and more efficient algorithms are needed based on results of chamber measurements randomly over time, as it is performed in this study.

3 Methods and experimental design

3.1 Field area description

3.1.1 Measurement site

The field experiments took place in summer 2014 from June 15th to August 20th in the Sakha region, Siberia, north-east of Russia (Figure 5, left) close to a tributary of Kolyma river. The channel system with the field site there is located 15 km south of Chersky at Ambolika river (68° 36' 47"N, 161° 21' 5"E).

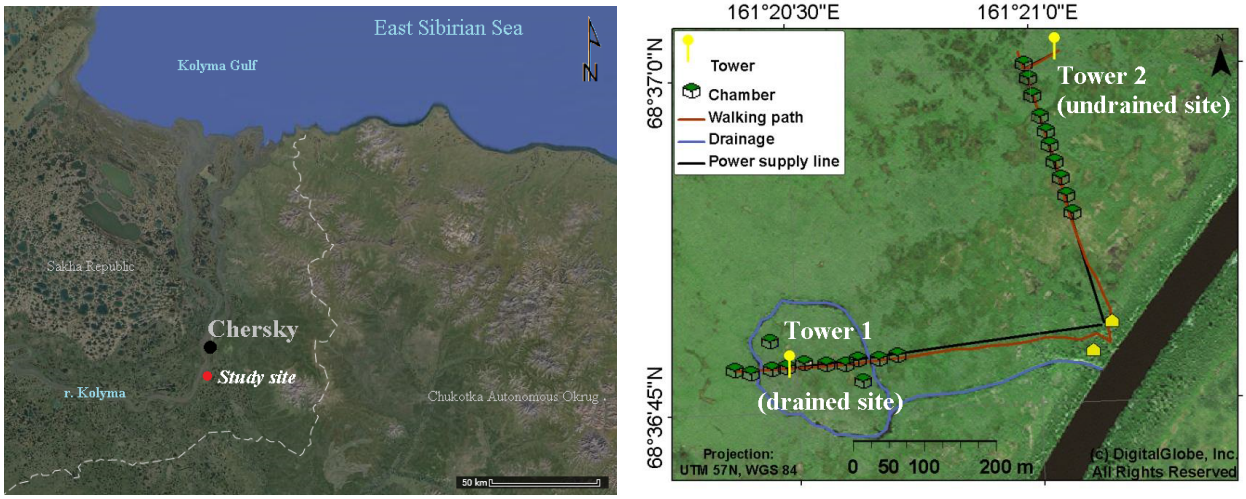

Figure 5: Map of the region near Chersky, north-east Siberia (left) where the study site is located (Imagery, 2014 Landsat, IBCAO, Map data 2014 Google) and experimental study site "German tower" (right) with drained and undrained (natural) transect (Kwon et al., 2014) near the Ambarchik river. Two additional big chambers with associated small chambers each are shown apart from the drained transect.

The study side is divided into two transects of chambers meeting at the worker's place on riverside (Figure 5, right). The drained transect (No. 1) lies in east-west direction and orthogonally to the river. The undrained transect (No. 2) lies in north-south direction. Both parts have ten chamber stations that are equidistanty distributed along 225 meters. The chambers are numbered from 0 to 9, where the furthest from the worker's place starts with 0 and numbers increase with decreasing distance. A detailed description is given in subchapter 3.2. Additional, two big chamber sites (B1/3, B1/7) about 200 cm x 200 cm x 60 cm with an additional common, acrylic chamber each (S1/3, S1/7) next to it were built within the drained area. Big chambers were made of wood, unsealed and not gas tight, since they used to be covered with a plastic tarp. In the drained transect only chamber 1/0, B1/3 and S1/3 was flooded and in undrained transect 2 only chamber 2/4 and 2/5 were dry. Additionally, an eddy-covariance-tower was built at each transect for the micrometeorological monitoring and for later comparison of CO_2- and CH_4-fluxes with chambers.

Disturbing influences by walking and stamping around at the field site concerning ebullition are minimised through a wooden boardwalk (Davidson et al., 2002; Kutzbach et al., 2004), especially while working with the chambers.

3.1.2 Climate and meteorology

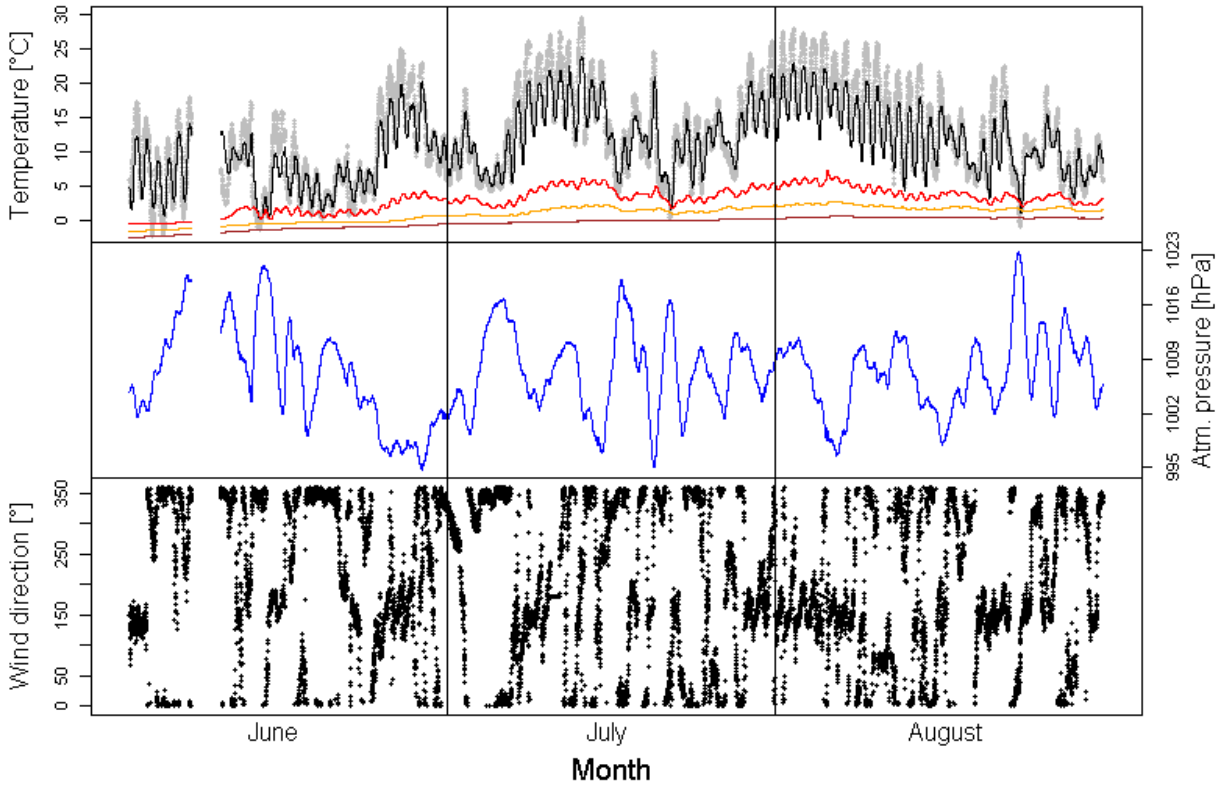

Figure 6: Graph of air temperature (grey crosses), soil temperature at depth: 4 cm (black line), 8 cm (red line), 16 cm (orange line), 32 cm (brown line), air pressure (blue line) and wind direction (black crosses; north: 0 / 360°, east: 90°, south: 180°, west: 270°) of the field site at tower 2 from June 1st to August 31st 2014. Between June 6th and June 9th data is missing.

Due to the location of the study site north of the polar circle the sun position in summer stays above the horizon, while in winter the sun appears merely a few hours per day depending on closeness to winter solstice. Therefore, weather conditions are changing noticeably throughout seasons. Short waved radiation rose up to 821 W m^{-2} at noon during meteorological summer 2014 with the maximum in the first half of June. Wintry river ice and snow can exist until June and appear in September again. Although, summery air temperatures can reach almost 30°C (Figure 6) average temperatures and air pressures of 11°C and of 1008 hPa, respectively, were measured during the field work in 2014. There are two main weather systems that affect the ambient conditions: (1) wind directions from north

bring lower air temperatures and higher air pressures from the polar anticyclone; (2) wind directions from south, bring high air temperatures and low air pressures. That means, air pressure, air temperature and wind direction are dependent on the weather situation and are linked with each other. Soil temperatures in the upper soil layers follow exactly the air temperature in daily cycles and decreases with depth. Upper soil layers thaw successively, while in 32 cm depth the soil stays frozen over summer (indicated by linear slope). Precipitation amounts are around 413 mm per year and the climate by Köppen at the site is classified as continental subarctic (CantyMedia, 2014), supported by data since 1957.

3.1.3 Permafrost and flooding

The past climate situation since the Pleistocene is the reason for large carbon stocks in the permafrost of northern Siberia (Zimov, 2005). During the spring melting of snow in May and June permafrost leads to the flooding of river planes in the studied area, as the river melts from the south and pushes an ice wall to the north, which dams up the melting water. Moreover, the melting water cannot infiltrate the soil in this situation. The thawing of the soil starts in the middle of June (Merbold et al., 2009).
Independent of snow driven flooding, standing water level occur annually due to thawing of frozen soil. With the thawing depth during the summer the active layer deepens (Figure 2, Figure 6), wherein CO_2 is metabolised into CH_4 by microbes (Merbold et al., 2009). During longer vegetation periods the active layer can deepen between years and the potential of converting CO_2 to CH_4 increases (Klapstein et al., 2014), in particular in later vegetation period. Therefore, the active layer depth (ALD) was taken with every measurement by pricking an iron pole into the soil as deep as possible to the frozen soil surface.
For analysis about dry artificial and wet natural conditions a drainage ditch was applied resembling to permafrost polygons with high levelled dry centres and low wet rims (Sachs et al., 2010). Due to flooding of large soil surface areas, incomplete humidification and low average temperatures around the year the decomposition of organic matter develops slowly. That leads to peatland conditions at the field site with flooded sites of standing water and dry sites without standing water on the soil surface, as well due to the drainage there. In September the mean water tables rise above the soil surface at the drained site (Merbold et al., 2009) up to the level of dry sites.
The yedoma peatland soils show loess characteristics (Zimov et al., 2006) and store large amounts of carbon and organic matter in these soils, which accumulated for millennia since Pleistocene (Zimov et al., 1997). Parts of this organic matter are transported into the river as DOC due to lateral movement. The studied area is flat and thus, no soil erosion is visible directly.

3.1.4 Vegetation

The growing season at the studied site turns out to be rather short with three months (Merbold et al., 2009) because of rough climate and short summer conditions. The biome there is classified as wetland tussock tundra (Merbold et al., 2009). At the biome border between boreal taiga forest and treeless tundra only needle-leaved larches grow at certain places on riversides and around mountains up to approximately 500 metres. The vegetation in the field site is often patchy with occurrence of different grasses, herbs and shrubs. The reason for this observation lies probably in slightly different altitudes where water is standing on soil or not. These differences range only within a few decimetres.
Most important plants for determining CO_2- and CH_4-fluxes in chambers were sedges (*Carex appendiculata*), which grow in typical tussock shape and *Eriophorum angustifolium* as a cotton grass (Figure A-1) that shows aerenchyma for gas conducting between soil and atmosphere (Merbold et al., 2009).
In flooding situations after snow melting merely a few plants are able to withstand the constant standing water level above soils. In most cases they have aerenchyma. Willows and cotton grass are physiologically adapted to standing water (Figure A-2), while tussock sedges annually grow again on the old stocks (Lawrence et al., 2013) and rise their own root environment above water level. Klapstein et al. (2014) found that sedges promote CH_4-production. In a normal flooded situation water decreases to a lower level in dry sites. Mainly shrubs such as willow (*Salix myrtillifolia*, *Salix pulchra*), birches (*Betula nana* subsp. *exilis*) and leatherleaves (*Chamaedaphne calyculata*) appear there. Their growing height seldom exceeds two meters. Between shrubs tussock occurs, together with herbs like marsh cinquefoil (*Potentilla palustris*), bluejoint (*Calamagrostis canadensis*), elephant's head (*Pedicularis groenlandica*) or golden saxifrage (*Chrysosplenium tetrandrum*), while in wet sites mainly and often exclusively cyperaceae (sedges) appear.

3.2 Chamber setups

Working with measurement devices in remote areas of north-east Siberia like in this study requires testing and preparation of materials and experiments. Therefore, test measurements in the Max-Planck-Institute of Biogeochemistry in Jena (Germany) were done to find and specify possibly successful chamber setups. The main focus on these test measurements was placed on the configuration of fans and distribution of the gas inside the chamber. These additional methods were independent of the field setup tests, that focused on the real gas emission out of the soil and how it changes with different configurations. The used devices are shown in Table 1. The setup of chamber measurements for detecting CO_2 and CH_4-fluxes is based on former works on this topic (e.g. Drösler, 2005; Tokida et al., 2005). For the

measurement of gases a closed dynamic system was used with technical properties of a non-steady-state flow-through chamber (Rochette and Hutchinson, 2005) to detect a cumulative flux (Tokida et al., 2005) and avoid much influences of the microclimate through low closing times, around two minutes. The sampling air circulated constantly between the chamber inside and a gas analyser.

Table 1: Sensors of test and field chamber setups.

Location	Test chamber (Laboratory)	Field chamber (north-east Siberia)
Inside chamber:	CH_4 (stationary)	CH_4 (portable)
	CO_2 (stationary)	CO_2 (portable)
	air pressure	air pressure
	air temperature	air temperature
	air humidity	air humidity
	Solar irradiance / PAR-sensor	Solar irradiance / PAR-sensor
Close surround chamber:	Soil moisture (ca. 10 cm deep)	Soil moisture *[out of order]*
	Soil temperature (ca. 10 cm deep)	Soil temperature at four depths (5, 15, 25, 35 cm)
	-	ALD

Dimensions and materials of field chambers are similar to these of the test chambers. Cubic dimensions of chamber walls were 60 cm x 60 cm x 60 cm. The chamber hood was constructed from acrylic for transparent conditions inside and fixed with frames in the chamber wall edges at test chambers, but were glued instead of screwed frames for a better tightness. The entire chamber hood stood on a collar buried in the soil with a rim about 15 cm high above the soil level and made of metal for test chambers. Field chamber collars were constructed of plastic and differed in the height because of different elevation. For getting a tight air chamber on the bottom near the gas emission the collar rim was filled with water, so gases could not escape as easily as without water in the rim.

3.2.1 Gas analyser

In test measurements a laboratory PICARRO G1301 gas analyser was used driven by an external pump. Results are visible online and plotted in a graphic software. The operation system works as a wavelength-scanned cavity ringdown spectroscopy (WS-CRDS) for CO_2, CH_4 and H_2O (Rella, 2010). In this process a laser (wavelength for CO_2 = 1603 nm and for CH_4 and H_2O = 1651 nm) is reflected by at least two mirrors several times inside the cavity while becoming absorbed and scattered by the test gas (Crosson, 2008). The reflected laser signal is captured by a photo detector. From the comparison of laser energy loss due to the test gas with reference values the final result is calculated. The precision of PICARRO

G1301 for CO_2 is under 200 ppbv / 50 ppbv (1 σ over 5 s / 300 s) and for CH_4 under 1 ppbv / 0.7 ppbv (1 σ over 5 s / 300 s), respectively (Picarro, 2011). The measurement frequency was under five seconds, the gas response under three seconds and the measurement range for CO_2 was between 0 and 1000 ppm and for CH_4 between 0 and 20 ppm, respectively. Data could be stored on the gas analyser device for the test gases. To protect data from physically ambient instruments an external data logger was necessary. The chamber inside and gas analyser were connected via 6 mm tubes and an adapter for $\frac{1}{4}$ inch to 6 mm.
For measuring at different sites an ultra-portable greenhouse gas analyser (UGGA) by LOS GATOS RESEARCH (LGR) was used. After the online analyses values were store in the device as well. The measurement technology is based on off-axis integrated cavity output spectroscopy (OA-ICOS), an improved method of CRDS for field usage. The operation is the same as for the PICARRO gas analyser. The accuracy of the UGGA is < 1 % $(10 - 35°C)$ and the precision for CH_4 is about 2 ppb / 0.6 ppb (1 σ over 5 s / 100 s), respectively. The measurement frequency was selected to be less than 1 Hz and the measurement range was set between 0.1 and 10 ppm. An additional portable data logger provided more safety for storing data. It was connected with a field netbook ALGIZ XRW by HANDHELD and showed immediate values for other logged data beside CO_2, CH_4 and H_2O of the UGGA like solar irradiance, air humidity, air temperature, air pressure, soil moisture and soil temperature. Chamber inside and gas analyser were connected like PICARRO gas analyser via 6 mm tubes and an adapter for $\frac{1}{4}$ inch to 6 mm, as well.

3.2.2 Test chamber measurements

In preparation for field measurements the test chamber under laboratory conditions had almost the same conditions like the field chamber. Bare composted organic material was put in a metal frame about 20 cm high underneath the chamber installation and growing seedlings were removed during the measuring period. For data sets with an obstacle as a tussock reconstruction inside the chamber dead brown leaves of a common garden yucca were used to avoid assimilation, respiration and transpiration of green plant material. Therefore, CO_2-fluxes could be used for the analysis. The leaves were approximately 46 - 60 cm high, in average 43 cm wide and stored in a 40 litre bucket. For simulating a natural gas emission behaviour the soil was irrigated at every evening before measuring so metabolism of microorganisms could work. Additionally, the sun radiation and heating up was avoided by building shadow inside the chamber with a moveable wall outside the hood.

Test chamber setup

The main chamber hood setup is already described in subchapter 3.2. In the chamber roof an open chimney ensured the import of optional wires and instruments. During the measurements the hole was closed with an elastic sealant. The PAR-sensor for solar irradiance (photosynthetic active radiation) in test chambers was portable but put on the soil at all measurements near the chamber centre if possible due to different setups, e.g. with or without plant obstacle. The wires led to an external data logger buried in the soil under the collar. Outside sensors were buried in the soil as well approximately 10 cm deep.
Ventilation and air mixing were highly important approaches for this study (Pumpanen et al., 2004) due to the usage of non-steady-state chambers and therefore, fans necessarily had to be implicated. For better handling with the chamber hood the 12-V-fans were fixed on a pole that stuck horizontally turnable in the soil permanently in a corner of chamber hood (Figure 7). Due to the absence of flooding and methanogenesis in the soil thereby no disturbance trough additional pathways were created. The fans were attached moveable with cable ties to experimentally alter the height and the distance between ventilation devices. Usually, fans at three heights were set at 15 cm, 35 cm, 55 cm. Against other setups with a vertical mixing between top and bottom (Pérez-Priego et al., 2010; Yu et al., 2014) here a transversal air stream was created (see Drösler, 2005).
Tubes for the inlet of gas from the chamber to the analyser were forked into three incomings for profile observations and were variably displaceable for different measurement sets due to the positioning at poles. For the outlet of gas from the analyser to the chamber a perforated plastic tube was fixed around the collar near ground at approximately $\frac{2}{3}$ of collar height.
Measurements were done three times each until two minutes of stable slopes were reached. An overview of the test chamber setup measurements is given in the results (Table 2).

Ventilation measurements inside the chamber

The main question about this topic was how to get a well air mixing inside the chamber (Pihlatie et al., 2013). There were several approaches to solve that problem, like distributing aerosols from smoke tablets inside the chamber to see an air stream and turbulence or fixing paper slices there on the walls and corners for watching more or less moving. But smoke spread to fast and built a homogeneous fog (that Müller et al., 2009 interpreted as fast mixing) and paper slices movement was not quantitative and too subjective. Therefore, a ventilation gradient may show the air mixing due to different wind speeds at certain points of the chamber.
The wind speed was measured with an one-dimensional hot wire anemometer for observations between 0 and 10 m s^{-1} with an accuracy of 0.03 m s^{-1} $\pm$ 5 % of mean. Measurement

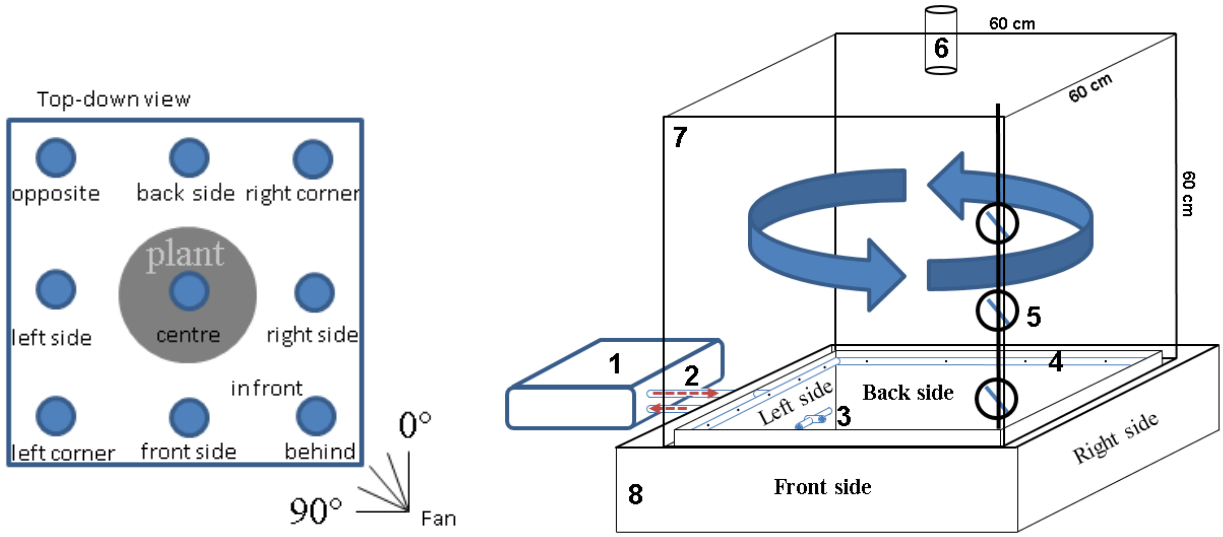

Figure 7: Two-dimensional test chamber scheme from above 60 cm x 60 cm (left). Blue dots show the positions of measurements inside the chamber, the grey circle means the plant bucket. Fan location was built between measurement positions "in front" and "behind". Three-dimensional test chamber scheme from front (right). Blue arrows symbolise air mixing, red arrows indicate the air stream from and to the analyser. 1: Analyser and data logger, 2: inlet and outlet tubes, 3: forked inlet tube system, 4: perforated outlet tube system, 5: fans with pole, 6: optional closed chimney, 7: chamber hood, 8: metal collar.

frequency was set to 1 Hz. The bulk of the anemometer is heated and detects a cooling due to wind chilling. Therefore, it does not detect either wind direction nor wind velocity and also reflected wind from chamber walls influences the measuring. The hot wire anemometer was fixed in the position on a pole, such that the bulk faced to the chamber roof. That was done because of practical reason for a better lifting of the chamber and excluding of mechanical wire disturbances around the bulk, with exception of the centre point when the plant obstacle was placed there. In this case the bulk faced the other way round to the soil introduced from the chimney. The creation of different wind speeds required the distribution of fans in three layers between the usual fan heights of 10 cm, 30 cm, 50 cm at heights 5 cm, 25 cm, 45 cm with each nine points in a quadratic pattern (Figure 7): four in the corners, four at the wall sides and one in the centre. Additionally, one reference observation without fans was done and another behind the fans in comparison to the one in front of fans. Every data point is the mean of five repetitions with each 60 measurements over 1 minute (1 Hz). Finally, out of these 27 positions a three-dimensional wind speed distribution gives an impression of the mixing regime inside the chamber. Different setups also showed different situations as seen in Table 3. At configurations with plants the upper layers (45 cm above ground) of the inside chamber air had the widest plant offshoots, but less mass density and resistance for wind, smallest in the middle layers (25 cm above ground) and mediated extensions in lower layers (5 cm above ground), but more wind resistance due to the bucket as stem imitation.

3.2.3 Field chamber measurements

Additional to the described chamber hood three fans were installed with the vertical distance of 20 centimetres to each other and fixed at a pole on the chamber wall together with all other devices. This procedure was done to avoid pathways for gases out of the soil, contrary to the test chamber setup, where the fans stuck in the soil and low fluxes were expected. Instead, the pole with three fans was part of the chamber hood and normal attachment of fan angles was 45° to a blank wall side in heights of 5 cm, 25 cm, 45 cm above the collar. Due to the radiation angle of the polar summer sun the sensors were fixed at a single chamber side and without shading the chamber interior. Every hole for the poles and cables were closed tight with sealing screws and sealant.
Inlet tubes for the gas flow from chamber to analyser were forked into four incomings at 5 cm, 20 cm, 40 cm, 55 cm to get an integrated profile over the whole chamber interior. The outlet tube for the gas flow from analyser to chamber was placed at the chamber roof. Both tube systems were fixed at the chamber and could be connected quickly to the analyser with adapters.

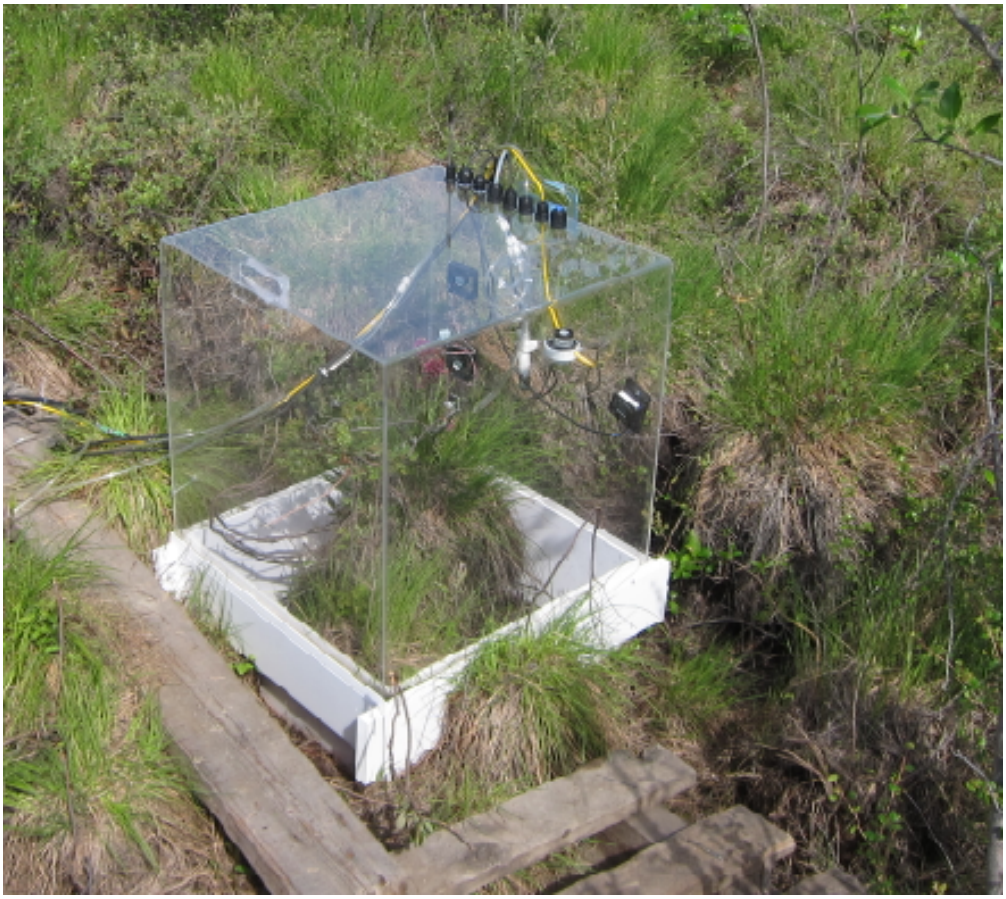

Figure 8: Field chamber with interior setup while NEE-measurement (photography by Carsten Schaller).

Another item for measurements of ecosystem respiration (ER) was the coverage with MYLAR foil to get an almost completely closed dark hood with values for PAR < 1 or even 0. Therefore, the foil was folded and taped to the shape of the chamber hood with a little wider material than the chamber to cover surely the entire interior. One corner was left unfixed to throw the foil quickly over the chamber for each measurement passage and form it into the right shape afterwards.

As described before in subchapter 3.2.2 of test setups the field measurements were done three times each until two minutes of stable slopes were reached to avoid overheating due to the greenhouse effect of the chamber walls. Since there is no useful method to detect the real natural methane flux during the measurements to find a stable ventilation and chamber configuration a definition of a reference flux was necessary. That is given by a normal setup, which was used in all of the other field measurements. This setup concludes out of the test measurements with three vertical fans 45° at heights 5 cm , 25 cm , 45 cm and a vertical inlet tube system at 5 cm , 20 cm , 40 cm , 55 cm placed at the front wall side. Compared to the normal setup several measurements with changed configurations of fans and inlet tubes were performed. Detailed measurements are shown in the appendix (Table A-5). All measurements worked as measurements of net ecosystem exchange (NEE) without darkening of MYLAR foil over the chamber for a better comparison. Thus, negative CO_2-fluxes are barely comparable with CH_4-fluxes, since NEE-measurements are dependent from plant activities due to solar radiation.

Chamber stations for the ebullition detection were located at the second transect with permanently flooded chambers and a dry chamber for comparison. To be more independent from coincidences a long-term measurement seemed the best choice, even if other studies observed far longer time periods over several hours, days and even months with different chamber systems (e.g. Christensen et al., 2003; Tokida et al., 2005; Yu et al., 2014). For that, regular measurements with three fans at 45°-angles to the wall side were set to one hour recording. Using longer breaks in field work a few extra long-term observations could be performed. Beside NEE-observations, ER-observations are done with MYLAR foil in dark conditions and have the advantage not to heat up due to sun irradiation while measuring. A possible disadvantage may be to miss the natural CO_2-flux that could influence CH_4 because of a lower gas conduction. However, the situation is disturbed while long-term measurements anyway and moreover Kutzbach et al. (2004) reported no relation between photosynthetically active green plant parts and plant-mediated transport of CH_4.

3.3 Mathematical data analysis

3.3.1 Flux calculation

The calculation of CO_2- and CH_4-fluxes is described by the following flux equation (combination of Kutzbach et al., 2004 and Pihlatie et al., 2013):

$$F = \frac{sl\ V_{Ch}\ p_{air}\ M_C}{R\ (273.15\,[K] + T_{air})\ A_{Ch}}\ \frac{60\,[s]}{1000\,[\mu g]} \qquad \left[\frac{mgC}{m^2\ min}\right] \tag{1}$$

Here the flux F is equal to the product of gas concentration change named as slope sl [ppm s^{-1}], the chamber volume V_{Ch} [m^3], the air pressure p_{air} [Pa] and the molar mass of carbon M_C [12 g mol^{-1}] divided by the product of ideal gas constant R [8.3144621 Pa K^{-1} mol^{-1}], ambient air temperature T_{air} [°C] and the chamber area A_{Ch} [m^2], multiplied with numeric factors for units. In preparation for the flux computation the data set is searched for a stable and suitable time window. Fluxes were calculated by bootstrapped slopes of the measured values without the first 20 s of initial phase of disturbed conditions due to chamber closing procedure. For that, a subinterval out of the whole 2-min-measuring was selected for the initial and for the final time of the slope determination. Possible slopes were calculated for several sections of this time window and the mean slope as well as uncertainty boundaries were statistically analysed.

3.3.2 Ebullition event evaluation

An ebullition event in the online gas measuring rises the current concentration slope for the time of emission and distributing with the chamber air (Figure 9). With a measuring frequency of 1 Hz of the LGR events ranging between 5 and 60 seconds within a 2-minute-measurement are detectable. When the bubble emission is over the slope continues the increase at the normal slope like before (Goodrich et al., 2011). Therefore, it is necessary to know what influences the distribution inside the chamber and how it works.
Further, the event size is given between different concentration levels and can be computed out of the difference of the final slope and the initial slope. For the evaluation of the flux change additional information are necessary about the measurement length, the surrounding conditions like air pressure, air temperature and the chamber volume (Equation 1). Then the emitted amount of CH_4 and the event fraction of the total emission is detectable. From that, the development of the event frequency, event length and event fraction during the summer period can be determined as well as the final event proportion of the CH_4-emissions at the studied site. The event duration window between the start and end time of an event is manually fixed at the last measured point that differs from the normal slope. The fraction

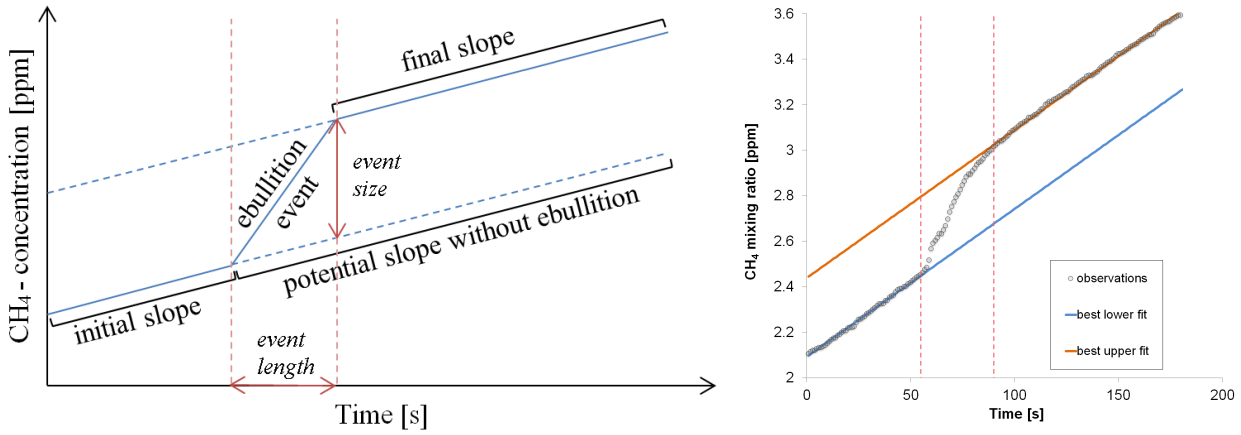

Figure 9: Diagram of an ebullition event with cumulative flux of closed chambers. Left: scheme. Blue lines indicate gas slopes, red lines indicate event properties (after Tokida et al., 2005). Right: example for a real measurement.

of an event shows the proportion of every single event to the mean total flux within the time of the measurement. For the final proportion of ebullition events to the total methane flux additionally the event frequency over the required time has to be determined and multiplied with the event fraction.

3.3.3 Statistics

For a reliable evidence about correlations and coherences a statistical analysis has been done with R version 2.15.0. The influence of environmental conditions on chamber setup measurements and between different chamber setups was calculated out of the comparison of mean gas fluxes (CH_4 and CO_2). Therefore, at least three repetitions per measurement were performed, although some values were defective, e.g. due to analyser failures. For that, a linear model was used that built the foundation for a statistical analysis of means with ANOVA, which computes statistical differences of mean values. The comparison of chamber setups via gas fluxes in different situations (water level, detected gas type, atmospheric conditions) worked with the normal-setup as reference. Additionally, linear fittings of ANOVA for mean fluxes with influence of environmental conditions were determined for every single setup and each of both gas fluxes. Some constellations of setup comparisons had merely few data or even no data and therefore give a weak view on influences or cannot be evaluated at all, but that does not mean there is no influence in this case.
The previously required normal distribution of datasets could be detected with the Shapiro-Wilk test. The influence of environmental conditions on ebullition events were performed with the Student's t-test for normally distributed data and the Wilcoxon rank sum test / Mann–Whitney U test for not normally distributed data.

4 Results and discussion

4.1 Test chamber measurements

4.1.1 Gas fluxes

The respiration activity inside the test chamber above the soil was low (Figure 10) compared to field CO_2-fluxes (Table A-5), since plants were missing. Regarding the diurnal course of fluxes there was a slight increase of fluxes without fans running (Figure 11, left) and no clear pattern with fans running as well as no significant difference between both configurations during daytime measurements. Thus, potential patterns in the diurnal course of respiration rates were considered negligible, and all flux rates were compared without further corrections, independent on what time of the day they were performed.

Table 2: List of flux measuring sets with the test chamber under laboratory conditions. Heights are scaled from soil surface. The occurrence of fans and an obstacle / plant are given in a separate column. Visualisation is shown in Figure 7. Measuring sets are listed in detail in the appendix (Table A-3)

No.	Description	Fans	Plant
-	Normal set for comparison: inlet tube positions in chamber centre at 10, 30, 50 cm; fan height at 15, 35, 55 cm; fan angle at 45° to chamber centre	with	without
1.	Different vertical inlet tube positions at each 5, 15, 30, 45, 55 cm	with, without	without
2.	Different horizontal inlet tube positions at each 10, 25, 40, 55, 70 cm	with, without	without
3.	Different fan combinations at each 1: 50 cm, 2: 30 cm, 3: 10 cm	with	without
4.	Different fan angles at each 0°, 22.5°, 45°, 67.5°, 90°	with	without
5.	Different horizontal inlet tube positions at each left corner, right corner, front side	with	without
6.	Different fan angles at each 45°, 90° and inlet tube positions at each left corner, opposite corner, right corner, front side	with	with
7.	Different fan angels at each 45°, 90°, different vertical inlet tube positions at each 10, 30, 50 cm and horizontal inlet tube positions at each right corner, front side	with, without	with
8.	Diurnal measurements (ca. 8 am – 6 pm) at five daytimes (morning, forenoon, noon, afternoon, evening)	with	with, without

The environmental conditions such as air pressure ($R^2 = 0.05$, $p = 8.4 \times 10^{-4}$), air temperature ($R^2 = 0.29$, $p = 2.5 \times 10^{-12}$), soil temperature ($R^2 = 0.29$, $p = 7.2 \times 10^{-14}$) and soil moisture ($R^2 = 0.22$, $p = 1.7 \times 10^{-10}$) showed a significant influence to fluxes. Air humidity or PAR had no significant influence. However, the correlation coefficient suggest a minor role of ambient conditions as also visible in Figure 10. More obvious was a longer stable phase with low mean values and standard deviations (SD), wherein even large variations of mean values and SD caused merely little altered fluxes. At the same time sets No. 3 - 6 (Table 2) had the lowest range of fluxes (Figure 11, right) when fans faced to the chamber centre and a vertical inlet tube system was used. However, the appearance of an obstacle, fan angles

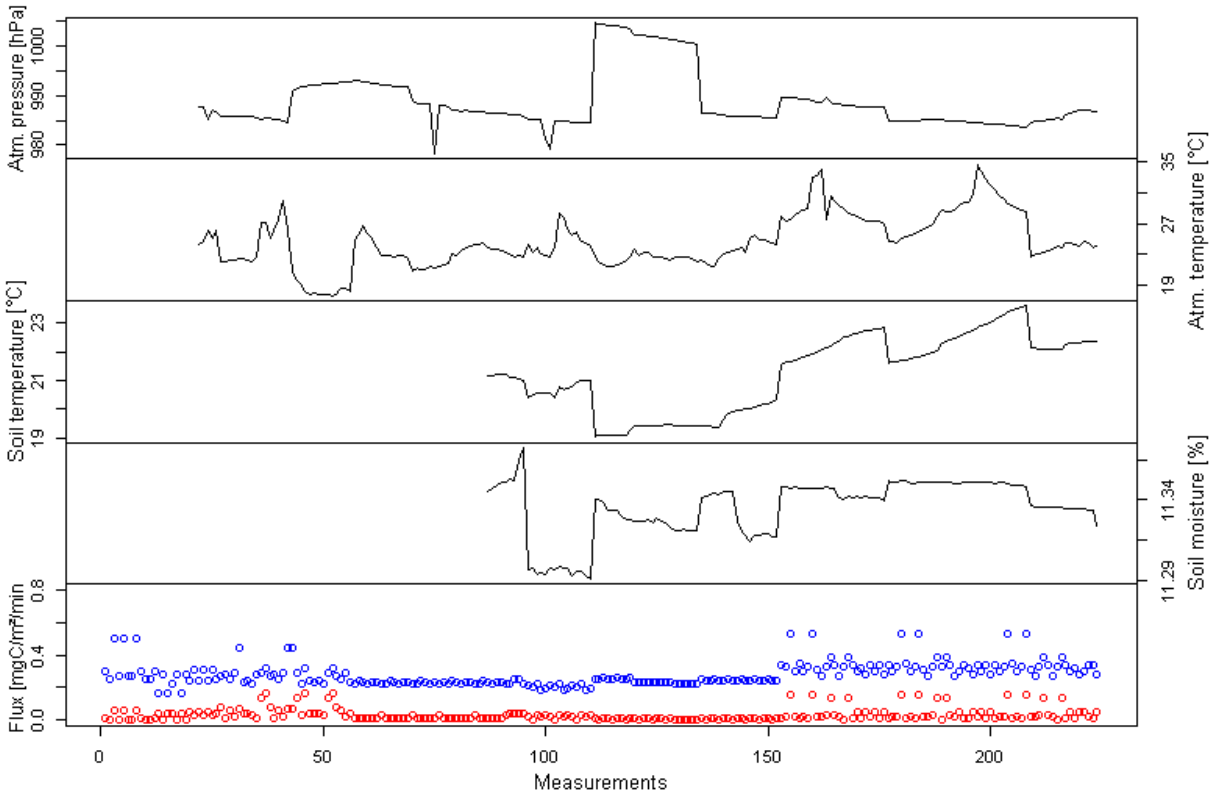

Figure 10: Test chamber CO_2-fluxes: Mean values of same configurations (blue dots), standard deviations (red dots) and environmental conditions (black lines) with significant influence on the flux. All test-measurements are shown that were taken from April 28th to May 23rd. The time series is plotted continuously with the measurements. Note the small scale for soil moisture, installation of air observing devices at April 29th and installation of soil observing devices on May 6th.

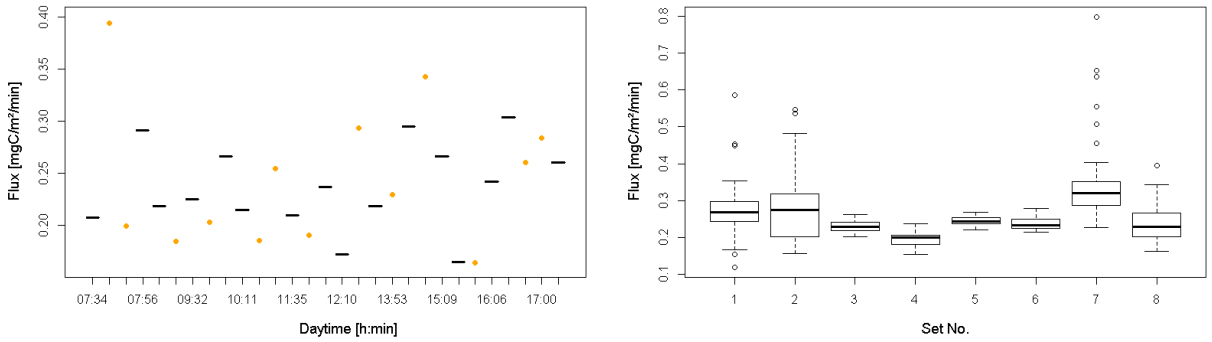

Figure 11: Diurnal CO_2-fluxes (left) of test chamber measurements with fans (black lines) and without fans running (orange circles) and of different setups (right; Set No. is described in Table 2).

and fan amounts have less influence on the flux change. Therefore, set 7 focussed on this difference with special configurations of different fan angles, vertical and horizontal inlet tube positions inside the chamber. Fluxes differed most and highly significant with different

inlet tube heights, if only one inlet tube height was used compared to two used inlet heights ($R^2 = 0.27$, $p = 8.2 \times 10^{-7}$) or three used inlet heights ($R^2 = 0.27$, $p = 2.2 \times 10^{-16}$) inlet tube heights. If the inlets were positioned in corners instead of wall sides ($R^2 = 0.50$, $p < 0.001$) and the deeper the inlets were placed fluxes differed as well, possibly due to worse mixing situation near the analyser air outlet. Another significant effect on flux changes occurred if no fans were used ($R^2 = 0.05$, $p = 0.04$), however, no significant influence of fan usage on altering air pressure could be found. Thus, several tubes for air inlets integrating the air sample vertically, placed between corners near fans and at least one running fan faced to any horizontal direction seems the best configuration for reliable chamber measurements under laboratory conditions.

4.1.2 Ventilation measurements inside the chamber

Ventilation measurements should show the air mixing inside a closed chamber. Therefore, different fan angles, air stream directions and occurrence of obstacles in the shape of a plant simulated different conditions. The variability of wind speeds gave in impression of well mixed, decoupled areas or even circulation patterns. Wind speeds ranged between 0.05 and 1.16 m s^{-2} and were around 0.02 m s^{-2} without fans in reference. Müller et al. (2009) had similar wind speeds of 1 m s^{-2} but with different ventilation system of radial blowers.

Table 3: List of inside ventilation measurement sets with the test chamber under laboratory conditions with SD for different heights. Fan heights are the same like for normal flux measurements, except No. 4 of ventilation measurements is similar to flux measurement No. 5 (Table 2). Visualisation is shown in Figure 7. Measuring sets are listed in detail in the appendix (Table A-4).

No.	Setup description	Fans	Plant	SD of upper layer	SD of middle layer	SD of lower layer	SD total
1.	Reference	3 x 45°	-	0.10	0.15	0.12	0.13
2.	Plant No. 1	3 x 45°	yes	0.12	0.15	0.23	0.19
3.	Plant No. 2	3 x 45°	yes	0.19	0.26	0.23	0.24
4.	Different fan angle	3 x 90°	yes	0.17	0.22	0.27	0.24
5.	Fans in different directions	2 x 0°, 2 x 90°	yes	0.11	0.13	0.32	0.24

High variations between repetitions of measurements with plants and fans in 45° to the chamber centre occurred especially for the positions behind the fans and in lower air layers close to the ground. With plants and fans in 45° wind speed was lower in many cases but spread over all layers compared to fans in 90° as well as the chambers without plants and fans in 45° (Figure 12). In case of exceptions the range from front side to right corner showed higher wind speeds for empty chambers, indicating an air mixing rather in flank corners of the fans than in the opposite. Thus, the plant seems to distribute the wind of the fans towards the flank corners. Lowest wind speeds without plant could be recognised with more remote distance from fans. With plants and fans in 45° lowest wind speeds occurred at the

opposite corner as expected for a setup with an obstacle in the centre.
To create a circled air stream around the obstacle fans were turned to 90° parallel to front side wall and in another case with each two fans parallel to both side walls (front side and right side) placed at the same corner. With three fans parallel to front side wall highest wind speeds of all configurations were reached with lowest speeds in the centre as Drösler (2005) found as well and highest speeds at the front side wall as well as in lower air layers. With two fans in two directions along both side walls around the fans the highest wind speeds occurred behind the fans, indicating a high suction from behind the four fans. Considering the SD of all five configurations the best mixing due to similar wind speeds existed without obstacles (Table 3), since no set with obstacle had comparable wind speeds in total. Thus, in lower layers wind flew faster, with largest differences between different locations inside the chamber and therefore with the highest expectable influence on flux measurements in field. Wind speeds in chambers with plants were most similar to empty chambers, if fans were turned 90° to wall sides and showed highest mean wind speeds of all configurations, which suggests a circulated air stream around the plant.

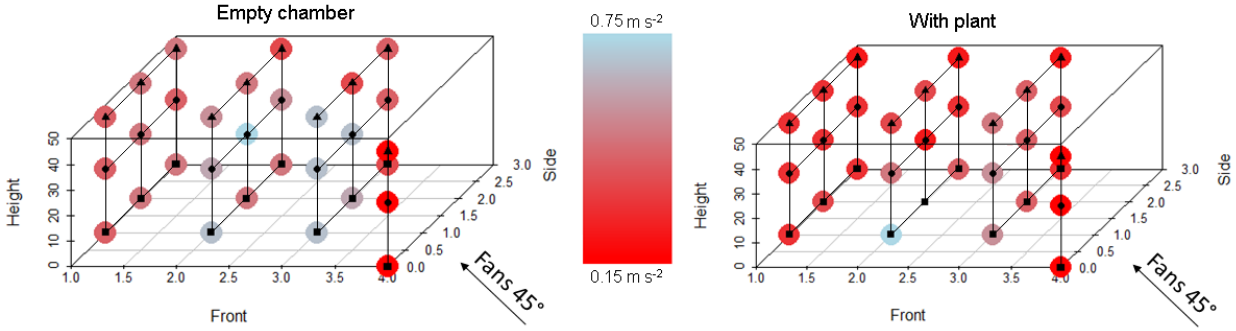

Figure 12: Wind speeds for chambers without plant, fans 45° (left) and for chambers with plants, fans 45° (right). With plant, fans 90° can be situated between both illustrations. Red circles indicate lower wind speeds, blue circles indicate higher wind speeds. The blank black square without colour (right) indicate the plant bucket without measurement possibilities. Fans were placed in the corner between front and right side.

Since at field sites highly variable shapes of tussocks and other plant species appear the results of these measurements cannot be generalised for field measurements, however, they give a reference for comparison. Thus, for an optimal reference with field measurements three fans should be used with the direction of 90° to wall sides to create a circulated air stream. Since with an obstacle every setup showed higher wind speeds close to the soil surface, only the reference set without obstacles lead to a better total mixing. Despite, with the fan direction of 45° to the wall sides this effect occurred less compared to other setups with an obstacle. Nevertheless, with each two fans directed into 90° and 0° to the side walls at the same time, a setup close to the reference without obstacle can be created, although the the lower layer showed the highest wind speeds. Therefore, at the latter configuration

fans in generally lower positions may help for a better total mixing over all air layers inside the chamber.

4.2 Field chamber measurements

4.2.1 Regular gas fluxes

The main manipulations (Table 4) presented the fan angle, which alter the air stream direction and thereby the air mixing. The experimental setups focused on three differences between fan configuration. The normal reference was a 45°-angle against the wall. The second one was constructed 0° straight to the opposite wall, which corresponds with 90° to the installed wall. Another setup with 45° in a horizontal transect to the soil surface and approximately 20 cm above the ground should simulated a positive air pressure. Furthermore, the inlet tube system was normally equipped with four openings in a vertical transect. Alternatively only two openings close to the ground instead of an integrating profile sim-

Table 4: List of chamber setups under field conditions and comparison with significant influence of atmospheric conditions with different gas fluxes. Setup No. 7 and 8 were considered separately. T: air temperature, p: air pressure. Percentage in brackets indicates the relative difference of mean values compared to the normal setup. Visualisation is shown in Figure 13.

Chamber setup configuration				Gas flux	
No.	Setup description	Fans	Inlet tubes	CH_4	CO_2
1.	normal setup	3 x 45°	4 in profile	$T^{(*)}$	-
2.	fan angles of 90°	3 x 90°	4 in profile	-	-
3.	no fans	-	4 in profile	low p, high T (-40 %)	$p^{(*)}$
4.	inlet tubes on ground	3 x 45°	2 on ground	-	$p^{(*)}$, $T^{(*)}$ low T (+35 %)
5.	inlet tubes on ground, no fans	-	2 on ground	-	$p^{(*)}$ low p, high T (-30 %)
6.	fans 45° to soil	3 x 45° to soil	4 in profile	high p, low T (+15 %)	low T (+45 %)
7.	fans on - off - on (1 min)	3 x 45°	4 in profile		
8.	fans on - off - on (2 min)	3 x 45°	4 in profile		

$^{(*)}$significant difference between all chambers

ulated of an immediate response without a mixing of methane with the chamber air. The alteration of wind and air streams in nature with an influence on gas fluxes should be imitated with intervals of running fans and no fans. It should show the impact of fans on the flux compared to fluxes in calm conditions. Besides, the turn back speed of gas fluxes with fans to a constant slope was assessable. This experiment considered three time phases: one minute of normal fans running, one minute without fans, one minute with rerunning fans. In another session the interval times were increased to two minutes.

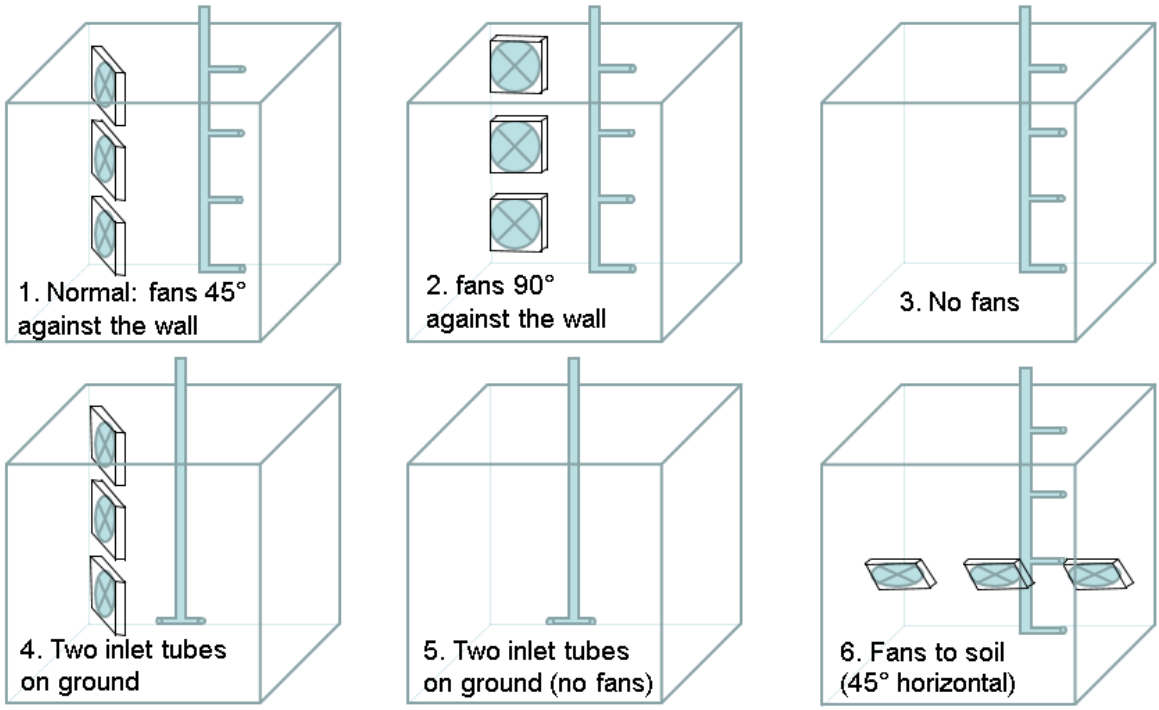

Figure 13: Different chamber setups explained in Table 4, excluding No. 7 and 8.

To detect a reliable flux with non-steady-state flow-through methods a constant slope of gas concentration is necessary. Due to the suspected independence of CH_4 from plant interactions like photosynthesis or respiration it shows a more constant slope than CO_2. That is the reason for using CH_4-slopes primarily (Couwenberg, 2009). On the other hand CH_4-production only appears under flooded conditions. That is why dry chamber stations are not analysable with CH_4-data.

The measurements were done over four days with different atmospheric conditions. Therefore, a comparison between chambers and with an influence of atmospheric conditions is possible. During these chamber setup measurements air pressure in summer was defined as low between 1005 and 1007 hPa and as high between 1013 and 1016 hPa; air temperature was defined as low between 7 and 10°C, as moderate between 17 and 23°C and as high between 27 and 36°C (no other values appeared). Therefore, the differentiation between the

measurements into several categories is appropriated: (1) influences of the chamber site; (2) influences of flooding; (3) influences of atmospheric conditions; (4) difference between CH_4- and CO_2-fluces. If the flux of a determined setup does not differ from the normal setup it may be considered as usable under the same conditions. For a simpler chamber setup and less sources of error the differences between air mixing through fans and gas sampling through profiled inlet tubes were tested (Table 4, Figure 13).

Influence of the chamber site

The results suggest different influences on CH_4- and CO_2-fluxes, such as chamber setups, chamber sites, atmospheric conditions and flooding situations. With focus on every single chamber site there was an influence of no-fans-setup about 39 % and fans-to-soil-setup about 15 % for CH_4-fluxes, compared to the normal-setup. In case of CO_2 except for the fans-90°-setup every other setup influenced the flux significantly from 18 to 57 %, compared to the normal-setup. CO_2-slopes were less stable than CH_4-slopes in general, i.e. more susceptible to changed setup conditions. For CH_4-slopes a higher flux appeared without air mixing due to missing fans. CH_4-fluxes significantly increased in this situation at one out of two chambers. CO_2-fluxes showed a different pattern and decreased significantly without fans in one out of four chambers. A similar pattern of decreasing fluxes occurred with the inlet-tubes-on-ground-no-fans-setup in two out of four chambers at the drained transect. Increasing CO_2-fluxes appeared with inlet-tubes-on-ground-setup, presumably due to the immediate transport with out-gassing. In these results an influence of fans is reflected because of the significant alteration of fluxes without fans, even if CO_2 is measured immediately with out-gassing without being dependent on mixing and metabolism of plants inside the chamber.

Influence of flooding

Considering wet and dry chamber sites there was no difference between setups with CH_4-fluxes nor under wet conditions for CO_2. Since there is no gas concentration slope at dry sites CH_4 cannot be evaluated. At wet sites the pattern of flux directions for different setups was similar for both gases, e.g. only no-fans-setup was lower than normal-setup. CO_2 showed a different flux for dry sites with inlet-tubes-on-ground-no-fans about 70 %. Atmospheric conditions ranged with $7 - 35$°C and 1006 – 1014 hPa too much to see an influence on fluxes, except for dry CO_2-sites. If positive pressure is produced with fans-to-soil a different flux is visible. These observations suggest that CO_2-fluxes at drier sites are merely slightly more dependent on the chamber setup. Thus, even though CO_2 is converted into CH_4 under flooded conditions via methanogenesis, the water level plays a minor role for CO_2-emissions due to far smaller amounts of CH_4-concentrations being metabolised out of CO_2.

Influence of atmospheric conditions

Considering atmospheric conditions mean CH_4-fluxes were generally lower by one order of magnitude with low air pressure and showed the most extreme values of all influences. Low air pressure and also high air temperatures caused significantly decreased fluxes about -40 % with no-fans-setup compared to normal setup that allow to conclude a poor mixing situation. In the opposite conditions at high air pressure and low air temperatures CH_4-flux increased about +15 %, especially significant for fans-to-soil. That is plausible if an artificial positive pressure multiplies the effect of high air pressure to maximise the gas emission through small ebullition (Yu et al., 2014), which was unrecognisable with the used analyser (the smallest analysable event in this study was 1,5 mgC m^{-2} d^{-1}). Otherwise a low air pressure or pressure drop should release more methane out of the fast responding upper soil layers (Tokida et al., 2005; Klapstein et al., 2014; Yu et al., 2014).
Also CO_2 showed strong negative fluxes about -30 % compared to normal-setup at low air pressure and weak fluxes at high air pressure situations, even though maximum values were not achieved. Here inlet-tubes-on-ground-no-fans had significantly lower fluxes and indicate a similar pattern as for CH_4-fluxes of less mixing without fans. Induced positive pressure through the fans-to-soil-setup revealed less low fluxes than the other setups, but not significantly. Comparing CH_4-fluxes with CO_2-fluxes it turns out that low fluxes occur with lower emission in case of CH_4 or even uptakes for CO_2. Increased fluxes with fans-to-soil emphasise this assumption.
A look at air temperature points out the significant influence of no-fans on CH_4-fluxes about -40 % for high air temperature, but fans-to-soil differs significantly about +15 % for low air temperature. CO_2-fluxes again show similar relations with significant influences about -30 % of inlet-tubes-on-ground-no-fans at high temperatures and about +45 % fans-to-soil as well as inlet-tubes-on-ground about +35 % for low air temperature, respectively. It means less CH_4 and more CO_2 appear, which manifests in a visible increase in CO_2 and a reduction of CH_4 by half an order of magnitude. However, lowest negative CO_2-fluxes at moderate air temperatures point in a different direction (Table A-5), because of dry conditions and thereby increased CO_2-production. The obvious difference between both dry chambers may lie in alternating plant composition with one third of willow, two thirds of sedge in contrast to the chamber with highest negative fluxes and 100 % sedge at lowest negative fluxes and therewith different CO_2-uptake between the chambers. But that is uncertain due to few data.

Difference between CH_4- and CO_2-fluxes

In general, comparing fluxes of CH_4 and CO_2 the setups show a similar behaviour for both gases (Figure 14), without significant differences. Despite, trends for lower fluxes through setups without fans and higher fluxes with induced pressure through fans facing to the soil are visible. While non of the setups showed a significant influence on CH_4-observations only inlet-tubes-on-ground-no-fans differed from normal-setup, but generally had few data. Compared to the other setups combining no-fans and the immediate measuring of unmixed and concentrated gases from soil in a lowered inlet tube system was the worst possibility for chamber configurations. Although it did not alter gas fluxes in every case, but CO_2-fluxes altered under different air pressures ($p = 0.03$) and as the only setup CO_2-fluxes differed with inlet-tubes-on-ground-no-fans from every other setup in general ($p = 0.01$). Even fans-to-soil showed no significant difference to the normal-setup, although high percentages of the air stream was probably reflected back into the chamber because of the 45° angle. Obviously, a less artificial setup is to tilt the fans against the wall instead of a tilt to the soil surface to avoid induced gas emission, especially at low air temperatures, high air pressures and dry CO_2-measurements. Concerning no-fans-setups the change of atmospheric conditions explain biases from the normal-setup for CH_4. In general CO_2-fluxes of this setup differed with air pressure ($p = 0.04$). In most cases gas fluxes from no-fans had lowest fluxes and were the opposite of fluxes from fans-to-soil with highest fluxes. With no-fans the vertical, horizontal and turbulent ventilation effects were excluded, i.e. no mixing of the chamber air appeared and gases accumulate close above the soil. This phenomenon was observed using inlet-tubes-

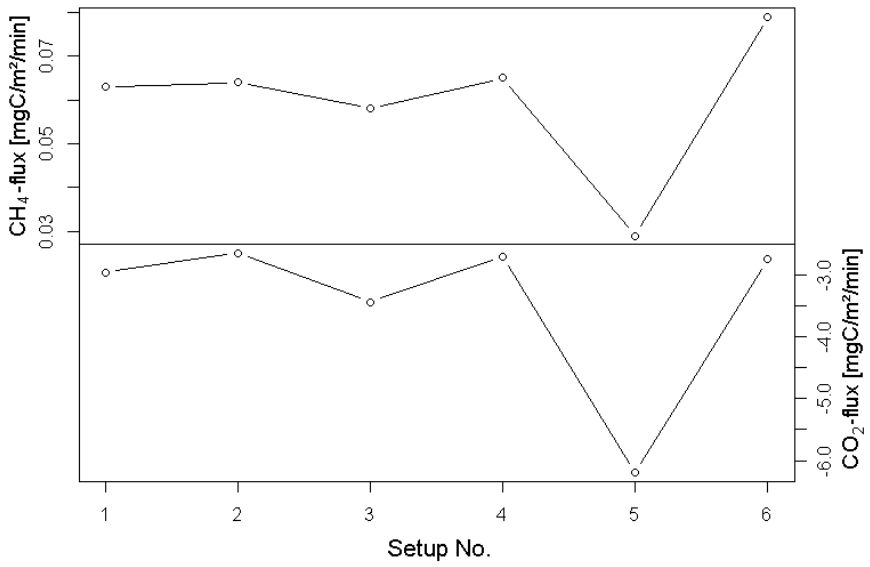

Figure 14: Sample for gas fluxes of CH_4 (only wet sites) and of CO_2 (wet and dry sites) with setups No. 1: normal, 2: fans-90°, 3: no-fans, 4: inlet-tubes-on-ground, 5: inlet-tubes-on-ground-no-fans, 6: fans-to-soil.

on-ground-no-fans-setup particularly for CO_2 that has a higher density than air and could not be verified for CH_4 with a lower density than air. However, between tussock structures and in slightly lowered terrain like flooded areas surrounded by tussocks a microclimate with reduced wind speed may support naturally poor mixed conditions and avoid methanotrophy due to less oxygen containing air (Goodrich et al., 2011).

Interval measurements with three phases

Turning fans off in between two phases of running fans is equal to the no-fans-setup for the CH_4-flux development and therefore comparable. The setup for phases of running fans was similar to the normal-setup. Thus, if gas fluxes were positive in phases without fans CH_4 accumulated faster and the pattern resemble artificial ebullition events (Figure 15). Negative fluxes indicate less mixed chamber air than with running fans and less emissions due to ventilation influences.
Comparing both phases of running fans (Figure 16) no difference appeared between before and after the calm phase. In some cases there were significant differences between phases of running fans and calm ventilation ($p = 0.03$), if the measuring time of each phase was long enough at least two minutes. With running fans the slope became linear even after a calm phase without running fans and went on at a similar level afterwards. The significant increase or decrease of slopes by initiating phase three with rerunning fans shows an immediate response of the slopes. That means, fans stabilised the slope in measuring periods, while

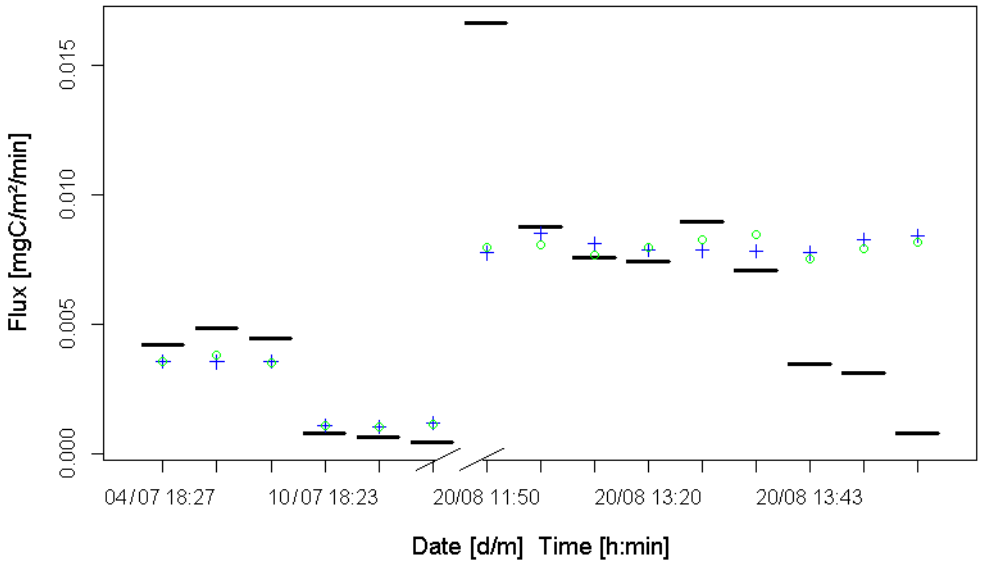

Figure 15: Chamber configuration with CH_4-flux over several days with phases of (1) running fans (blue crosses), (2) calm ventilation (black lines), (3) rerunning fans (green dots). The break of x-axis separates different measuring periods (left: July; right: August).

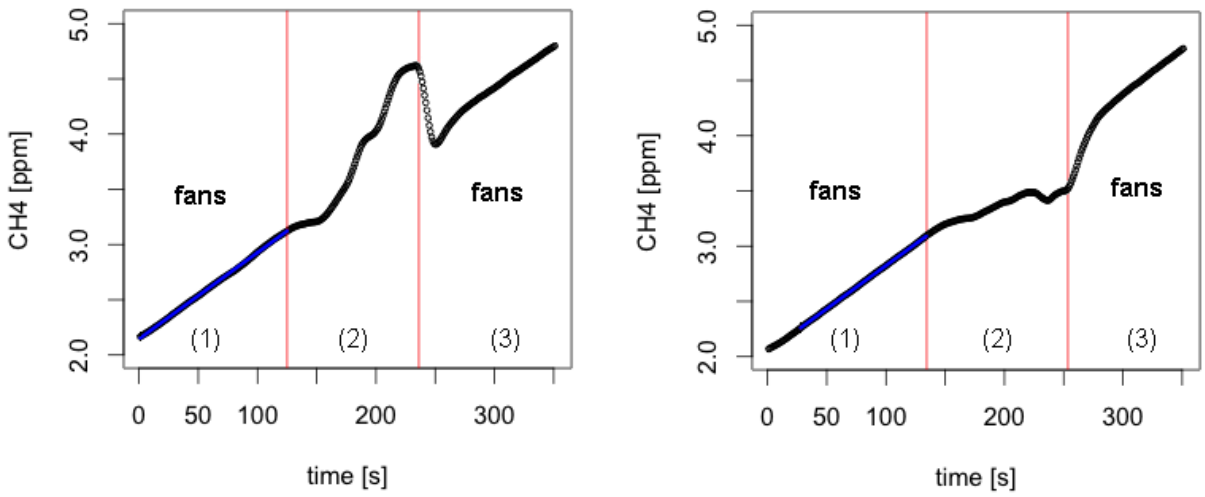

Figure 16: Interval measurements of two minute slopes per phase with three phases of (1) running fans, (2) calm ventilation, (3) rerunning fans, with initial slope (blue line) and interval borders (vertical red line) Left: positive slopes during calm ventilation, right: negative slopes during calm ventilation.

observations without fans differed significantly due to overestimation or underestimation if measuring times were long enough, i.e. longer than one minute.
Since there is insufficient data a significant influence could not be certainly verified. But under this circumstance, while no fans are running, slopes were significantly influenced by air temperature.

Summary of chamber setup measurements

Maximum flux values often appeared with fans-to-soil and fans-90°. Minimum flux values appeared with inlet-tubes-on-ground-no-fans and no-fans. With additional influences of artificial setups on certain conditions and different or even opposite directions of fluxes compared to normal-setup it may be possible to define boundaries of fluxes wherein the natural flux exists. These boundaries could be given in this evaluation by no-fans and fans-to-soil, even though there are no certain values detectable for either minimum or maximum fluxes.
In case of inlet-tubes-on-ground with normal fans running only one situation showed increased gas fluxes for CO_2 under low air temperatures. Otherwise no distinctive differences to normal-setup occurred, unless under different air pressure ($p = 0.002$) and air temperature ($p = 0.03$). For fans-90° no differences were visible. Thus, this setup is most insensitive to the surrounding conditions. That indicates a good air mixing inside the chamber, but does still not reveal whether these measurements with a fans-90°-setup really correspond to natural field conditions. In contrast even fluxes of the normal-setup differed under air temperature ($p = 0.03$). Hence, in conclusion fans were necessary for the air mixing and

ensured a reliable signal from both gases, with higher (CO_2) and lower (CH_4) density than air. The results of the interval measurements support this conclusion, since most unstable fluxes appeared in calm phases without running fans stabilised quickly after turning on fans again. Creating an horizontal air stream circulation inside the chamber could avoid positive pressure in contrast to vertical air streams and should mind the plant in the centre as an obstacle.

Considering atmospheric conditions both gas fluxes are significantly dependent on air pressure (CH_4: $p = 0.004$; CO_2: $p = 0.006$) and in the case of CO_2 additionally for air temperature ($p = 0.05$) but not for PAR, in contrast to Müller et al. (2009). That means, fluxes are affected by atmospheric conditions in many cases and in order to get a comparable gas flux similar measurement situations are necessary.

In comparison to test measurements with field measurements fan angles created an improved stabilisation of fluxes and therefore more reliable results, in contrast to the findings of Davidson et al. (2002). Due to respiring plants under field conditions fluxes became unstable and mixing through fans played a more important role in closed chambers (Christiansen et al., 2011), particularly in a dynamic system because of saturation effects. In both cases of laboratory test situations and field situations the integrating inlet tube system with a vertical gradient and fans 90° to the wall stabilised the gas sampling.

4.2.2 Ebullition events

Table 5: Event classification. Classes 1 - 5 were used to analyse events, class 7 was only partly assessable.

Quality	Event description
1	isolated event
2	multiple, isolated events
3	isolated event within different slopes
4	multiple, isolated events; but one incomplete event (initial / final slope)
5	after cutting of first 20 seconds: incomplete event (initial slope), probably artificial
6	incomplete event (initial / final slope), probably artificial
7	no stable slope
	Additional quality (event size)
	common event (< 0.1 ppm)
+	strong event (0.1 – 1 ppm)
++	very strong event (> 1 ppm)

To evaluate an ebullition event it is necessary to define the duration and the flux change (Figure 9) compared to the gas flux before and after the event. That is why an isolated event and sufficiently long gas slopes are needed (Goodrich et al., 2011). Hence, the ebullition analysis contained different qualities from a perfectly analysable, isolated, single event

to several, not clearly determinable events between unstable slopes (Table 5). Ebullition patterns were therefore manually detected out of the 2-min-slopes, but improved automated algorithms probably find events more precisely and faster in the near future.

Event frequency

Event frequencies are calculate by dividing the number of events by the number of measurements at a single day. Ebullition and other kinds of gas emission mostly occur in summertime during vegetation periods. There might be little amounts of diffusion through wintry snow cover (Friborg et al., 1997), but bacterial and plant activities are by far higher between snow melt and snow fall from June to September due to higher water levels and temperature (Christensen et al., 2003). Since in first parts of June the active layer was still shallow, the first half of the month almost no events appeared (Figure 17). July and August developed rising event incidences as Klapstein et al. (2014) already described and suggest ebullition in late summer season to occur rather due to permafrost thaw than to recent plant production. That could be the reason for the occurrence of an event with almost every second observation in this study in August. Also Yu et al. (2014) reported about increased event frequency with longer incubation time in the laboratory and Goodrich et al. (2011) assumed increased CH_4-production and less solubility. Not-analysable events and permanently dry sites are excluded in this consideration as well as long-term measurements due to varying frequencies throughout different measuring conditions.

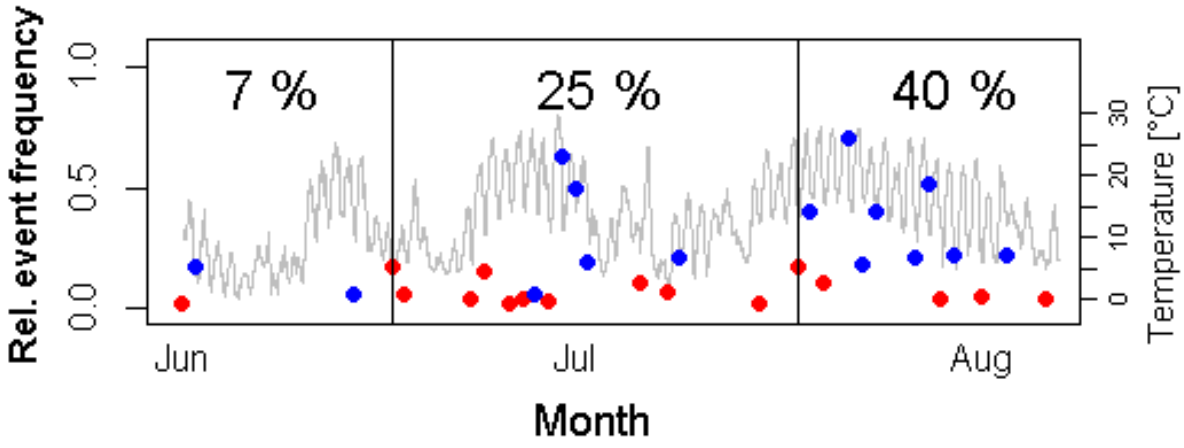

Figure 17: Relative ebullition event frequency (events per 2-min-measurement at a single day) of summer period 2014 from June 15th to August 20th at both transects (wet and dry sites), also written out in mean percentages per month. Blue dots encode more than five events per measurement at a single day, red dots encode less than five events per measurement at a single day, grey line shows air temperature. Vertical lines show 1st day of the months.

During a single day no specific diurnal course of fluxes occurred (Figure 18). There are only a few observations in the night, such that correlations were not strong for interpretation, while daytime observations were the general case of measuring and can be compared properly. Night and day were defined by explicit observations with lowest sun angles from 8 pm to 6 am. The absence of diurnal patterns suggests less variation of environmental conditions or important process cycles, unless too few events were detected to model a daily cycle. However, if bubbles form in deeper soil layers, the daily cycle is not influencing ebullition to the atmosphere. Besides, the summer sun remains even in the night above the horizon and rises throughout daytimes merely within little increased angles to ground. However, the diurnal influence is still visible in periodic air and soil temperatures (Figure 6). Yu et al. (2014) reported about increased ebullition during daytime of the laboratory experiment, while Friborg et al. (1997) only found diurnal variations during snow melt in subarctic peat and Goodrich et al. (2011) had no pattern in temperate peats.
Concerning every single chamber the wet sites had far more events than dry sites, due to their increased methane production according to the higher water level under undrained conditions. No events were observed in case of dry soils, with an exception of big chamber B1/7. At wet sites, 1 to 6 % of measurements within a single day featured an ebullition event at the drained site, while 6 to 41 % incidence at undrained site occurred.

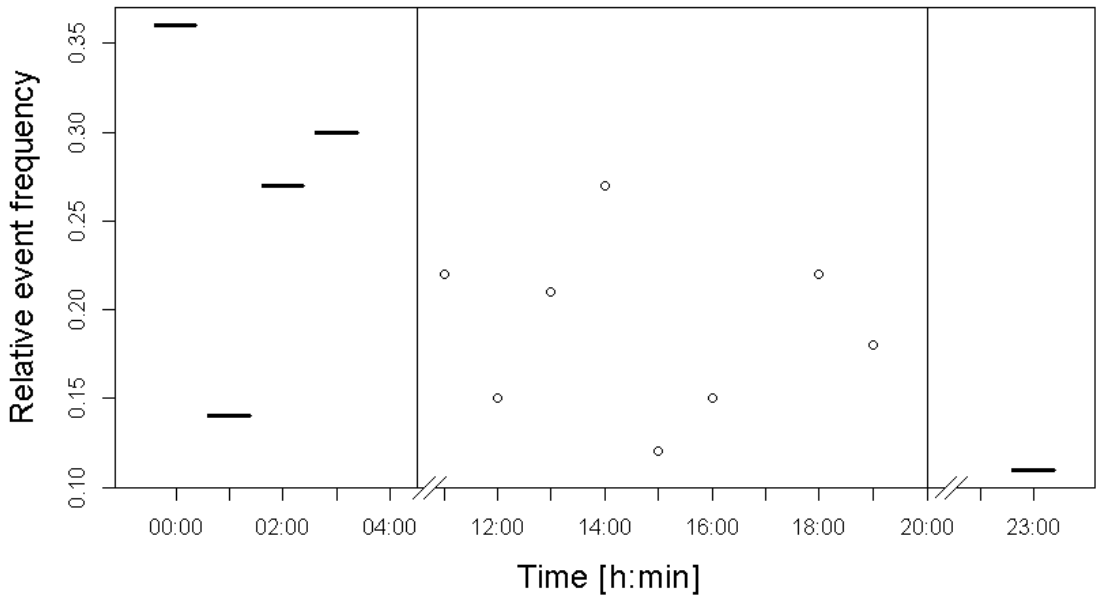

Figure 18: Diurnal relative ebullition event frequency (events per measurement at a single day) in the summer period 2014 from June 15th to August 20th at both transects (wet and dry sites). Circles encode daytime observations with more than five events per measurement at a single day, lines encode night observations with less than five events per measurement at a single day. Vertical lines show demarcation between day and night. The break of x-axis separates night and day

Event properties: size, fraction and length

Event sizes as absolute values of emitting methane bubbles [ppm] also describe the relative fraction of total fluxes. The partitioning of events into three classes (common: < 0.1 ppm; strong: 0.1 - 1 ppm; very strong: > 1 ppm) helps to distinguish between different strength, even if smaller events than 0.01 ppm exceeded the analysable resolution to divide ebullition clearly from noise. Yu et al. (2014) reported increased fluxes and found more weak events in their *Sphagnum*-experiment compared to this study with more stronger events (n = 78) than common events (n = 51) or very strong events (n = 3). The event length describes the duration of methane bubble emission and shows a good correlation to event sizes and fractions (Figure 19). In fact with longer event durations also event sizes grow, i.e. the strongest bubbles last longest. That is expectable because bigger events need more time for mixing with ambient air. Event fraction and length increased with stronger events (Figure 20). That means, with a higher, relative fraction of ebullition on the total flux absolute strength and size increased as well ($R^2 = 0.51$, $p = 2.2 \times 10^{-16}$) and have their maximum values during July (Figure 21). Sachs et al. (2010) reported same flux patterns for northern Siberia with similar dry and wet situations due to polygon structured micro hills and rims, respectively. In August mean and maximum values drop again as well as temperatures (Figure 17), which indicates the dependence of ebullition formation on the vegetation period.
Both transects show similar event sizes and event lengths without significant differences to each other. Event fractions (mean: 20 %) ranged between 6 to 60 % of total flux at transect 1 and between 3 to 78 % at transect 2, respectively. Event lengths (mean: 22 s) ranged from 3 to 51 seconds at transect 1 and from 2 to 72 seconds at transect 2, respectively. Despite, wetter or drier conditions do influence event properties significantly such as size ($p = 0.0001$) and length ($p = 0.04$). Air pressure was low with high event fractions, however, it was not significantly correlated with a generally low air pressure nor did it decline, as Coulthard et al. (2009) wrote.
An unexpected effect appeared to the distribution of event size and length over the summer, because both decreased at every transect from June to August, while event frequency and methane flux increased. Absolute values of event sizes, fraction and length increased until the second half of July, while mean values decreased (Table 6) due to only three data points in June. Thus, largest and longest events appeared in late July. The growth of total fluxes therewith was higher and faster than the growth of ebullition in beginning and end of summer, while ebullition fraction and event fluxes showed their maximum in second half of July. Probably, the process of bubble forming lasts a certain time before releasing at a certain threshold of 10 - 16 % by volume methane in the soil gas phase for smaller events (Yu et al., 2014) and after temperature increase, but slows down with temperature as well. Hence,

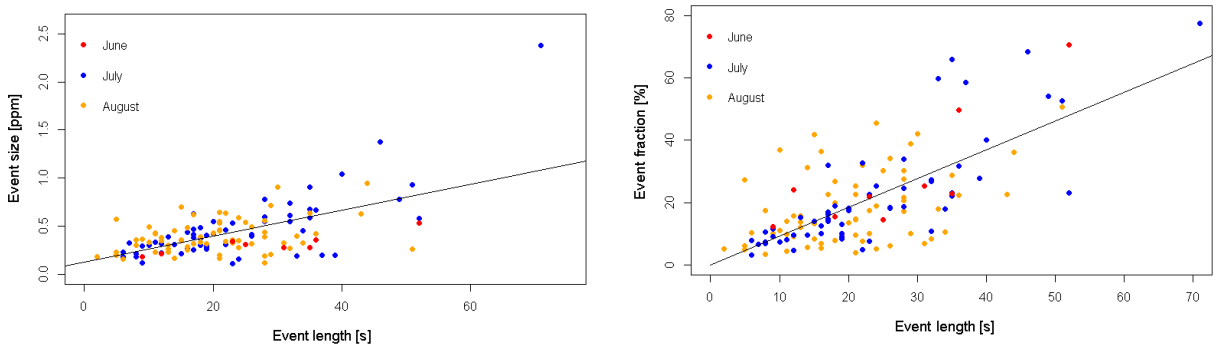

Figure 19: Correlation of event length with squared event size (left) as well as regression (R^2 = 0.35, p = 4.1 x 10^{-14}) and event fraction (right) with normal regression (R^2 = 0.47, p = 2.2 x 10^{-16}) for both transects, partitioned from June 15th to August 20th 2014 .

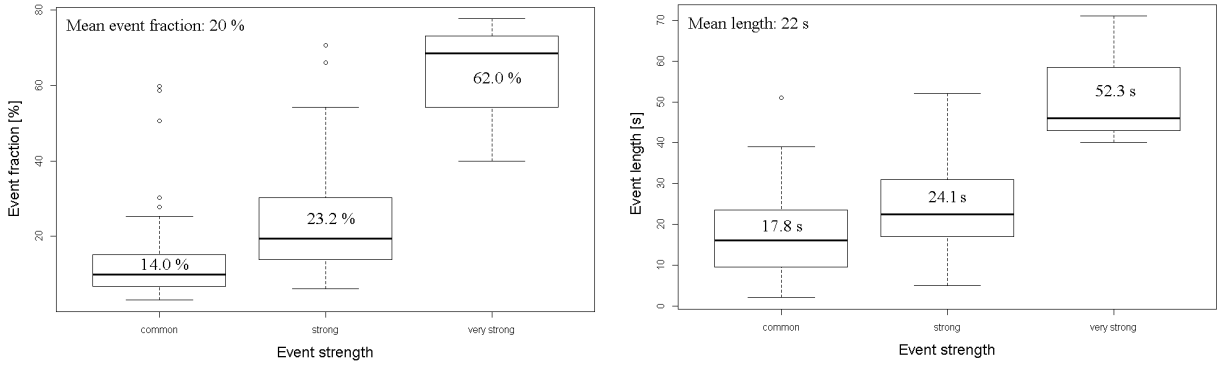

Figure 20: Coherence of event strengths with event fraction (left) and event length (right) for both transects from June 15th to August 20th 2014. Solid lines in box plots indicate mean values between second and third quantile. Dashed zones with error bars indicate first and fourth quantiles. Circles indicate outliers. Numbers show mean values. Common: < 0.1 ppm (n = 51); strong: 0.1 - 1 ppm (n = 78); very strong: > 1 ppm (n = 3). Note that event fraction is not equal to event proportion, but to event flux on total CH_4-flux.

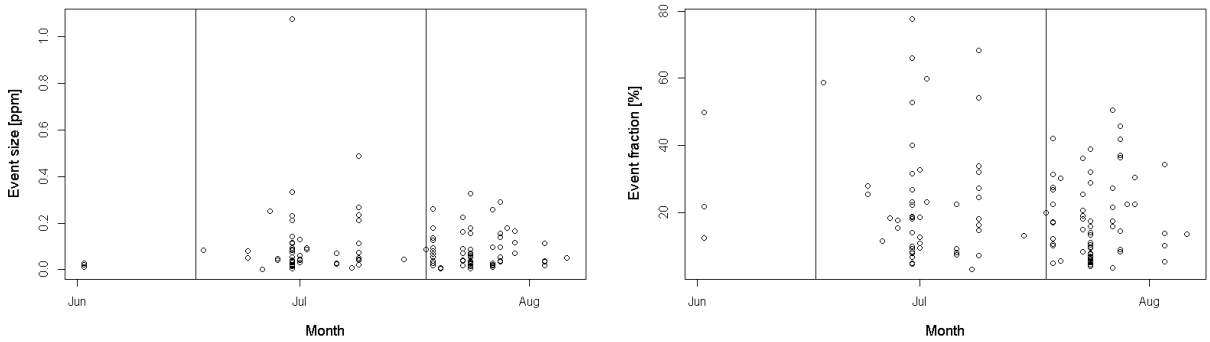

Figure 21: Development of absolute event sizes (left) from June 15th to August 20th 2014 at both transects (wet and dry sites) and relative event fractions (right).

because event fraction and length are correlated (Figure 19) the event durations decrease in August as well. Contrary to this, total fluxes kept on rising until August, but with an obvious decline in late July. The other pathways like diffusion and plant-mediated transport may be slightly less dependent on temperature.

Ebullition flux

Event fraction and event frequency are necessary for the determination of the final ebullition proportion on the total flux (Table 6), since in this study several measurements were taken instead of one continuous measurement. On drained and dry sites almost no ebullition occurred and thus, ebullition events there were considered in combination with transect 2 (flooded site). Because of lower water and therefore generally lower methane production at wet sites of transect 1 (drier site), both transects together showed lower values for total methane fluxes and ebullition proportion. Transect 1 had generally significantly lower methane emissions than transect 2, in difference -140 mgC m^{-2} d^{-1} compared to -180 mgC m^{-2} d^{-1} of Merbold et al. (2009) about ten years before. The development of ebullition proportion over the summer season showed an increase from June to August with the absolute maximum of 7.1 % in August at the flooded sites. Extreme events appeared in July with up to 28.1 % ebullition proportion at wet sites (Figure A-6). The growth over summer was equivalent for both considerations of the two transects together or transect 2 alone, due to the little influence of few events and few wet sites of transect 1. The decline in the second half of July is influenced by the same local minimum like for the event frequency values. In contrast to event frequencies the event fractions reach a maximum in the second half of June, apart from the global maximum in June with three measured events only. Also Yu et al. (2014) noticed an increased event frequency with lower event fractions. The ebullition proportion for each single chamber (Table A-6) cannot be taken for reliable conclusions because of individual conditions at each site causing large variations and in some cases only one observed underlying event. The influence of vegetation was visible especially for flooded sites, where mainly cotton grass occurred in 7 of 13 cases and sedges merely in 2 of 13 cases. Consequently, CH_4-emissions were found to be strongly dependent on the predominating vegetation (Kutzbach et al., 2004). Conspicuously, single ebullition proportions at transect 2 in July were higher than in August. That phenomenon appeared mainly due to the statistical population of values with less measurements in August, that was enhanced by increased event fractions in July (Table 6).

Flooded soil conditions in the Chersky region are closer to natural methane fluxes and have higher total fluxes on average of 410 mgC m^{-2} d^{-1} over the summer season, higher ebullition proportions on average of 6.1 %. Ebullition fluxes ranged from 2 to 1100 mgC m^{-2} d^{-1} in

Table 6: Ebullition flux (proportion of total flux [%]) and total methane fluxes. Transect 1: mostly dry sites, transect 2: mostly wet sites.

Observation type	Partitions of summer season	Ebullition proportion [%]	Event frequency [%]	n_{events} / $n_{measurm.}$	Event fraction [%]	Total CH_4-flux [mgC m^{-2} d^{-1}]
Transect 1 + 2 (wet and dry sites)	June	1.1	4.2	3/80	28.0	85
	July	3.5	15.6	50/340	23.5	364
	1st - 15th	4.0	19.5	32/176	21.9	392
	16th - 31st	2.7	11.5	18/164	24.6	319
	August	5.0	31.1	66/238	18.2	414
	Total	3.7	18.1	119/658	20.7	385
Transect 2 (wet sites only)	June	2.0	7.0	3/43	28.0	85
	July	6.4	28.8	44/153	22.1	366
	1st - 15th	6.5	32.5	27/83	20.1	389
	16th - 31st	5.5	24.3	17/70	22.5	332
	August	7.1	41.8	56/139	17.6	459
	Total	6.1	30.7	103/335	19.8	409
Long-term(*) (Transect 2)	June	1.3	4.5	8/194	28.8	110
	July	0.7	7.0	9/102	10.3	130
	August	0.7	4.9	1/5	14.6	490
	Total	0.9	9.7	18/501	19.9	141

(*)recalculated from 60 min to 2.5 min of measurement

this study, comparable to the whole range of recent values (Yu et al., 2014). The amounts of total carbon emission from the soil to the atmosphere in the summer season were found to be as high as the upper flux range of 1 to 640 mgC m^{-2} d^{-1} of Subarctic tundra and wet meadow tundra (Whalen, 2005). These carbon fluxes are more characteristic for episodic events with higher amounts of 70 to >1200 mgC m^{-2} d^{-1} and come from deeper soil layers than steady-state events (Coulthard et al., 2009; Yu et al., 2014). Ebullition proportion ranged over the summer from 1 to 7 % at wet and dry sites with mixed plant compositions of mainly sedges and cotton grass. These values are comparable to those of Windsor et al. (1992) and Martens et al. (1992) who estimated 7 - 22 % in the Subarctic and < 1 - 17 % ebullition proportion in the Subarctic tundra and drainage ditches, respectively. Thus, with rising fluxes the proportions of ebullition increase to the maximum in August as well.

At sites with an occurrence of vascular plants the detection of an influence from plant-mediated transport on ebullition appearance due to higher proportions to the total flux (Whalen, 2005; Fritz et al., 2011) and less methane through diffusion must be the next step to provide reliable evidence for proportions of different pathways in the studied area. Almost every flooded site showed high proportions of cotton grass, beside the chamber site 2/0 and 2/3.

Coherence of ebullition with environmental conditions

Since no clear statistical correlations could be found on ebullition dependency from environmental conditions, the difference between situations with and without ebullition has been regarded. In this consideration influences on ebullition were determined by different parameters (Table 7), however, with correlation coefficients $R^2 < 0.1$. That means, ebullition appearance is still unclear to predict, although strong dependence on CH_4-fluxes occurred for event sizes ($R^2 = 0.81$, $p = 2.2 \times 10^{-16}$), but not for event frequencies, i.e without specific patterns.

Table 7: Coherence of ebullition appearance with environmental conditions. Only significances ($p < 0.05$) are shown, since always R^2 was < 0.1, beside the correlation of CH_4-flux and event size with $R^2 = 0.81$.

Parameter	Event size	Event frequency
Air pressure	$p = 1.5 \times 10^{-7}$	$p = 0.048$
Air temperature	$p = 7.2 \times 10^{-3}$	-
PAR	-	-
CH_4-flux	$p = 2.2 \times 10^{-16}$	-
Active layer depth (ALD)	$p = 1.5 \times 10^{-5}$	-
Soil temperature 5 cm	-	-
Soil temperature 15 cm	-	-
Soil temperature 25 cm	$p = 4.5 \times 10^{-3}$	-
Soil temperature 35 cm	$p = 1.4 \times 10^{-4}$	-

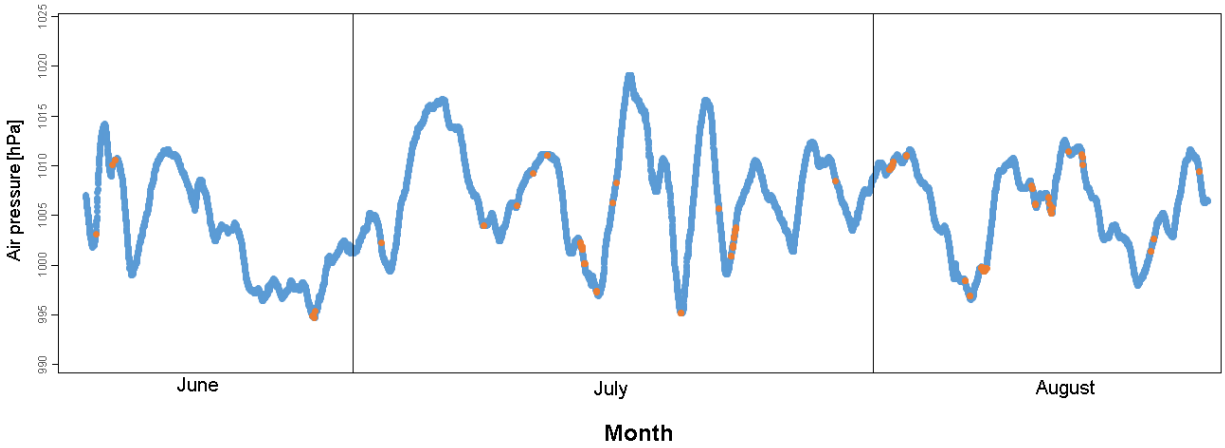

Figure 22: Coherence of air pressure and event occurrence from June 15th to August 20th 2014 at both transects (wet and dry sites). Blue line indicate air pressure, orange dots indicate ebullition events. Vertical lines show the first day of the month.

Temperatures in the atmosphere and deeper soil layers of 25 cm and 35 cm depth significantly influenced event sizes, in contrast to more shallow soil layers. Thus, in case of an air temperature increase also the soil heats up and more methane will be produced through methanogenesis. That happens particularly close to the frozen ground (Klapstein et al.,

2014). The expectations suggested temperatures in shallow soil layers to influence ebullition events because of a faster response to air temperatures. Out of the same reason the active layer depth influenced the event size. Hence, the influences of deeper soil layers at 25 cm and 35 cm depth mean increased thawing, spreading of the active layer and release of old carbon, as also found by Klapstein et al. (2014). Evidently the event frequency was connected to temperature of atmosphere and soil (Figure 17), however, with respect to the low correlation coefficients this influence seemed very small.
PAR showed no significant influence on ebullition, even though plants with aerenchyma may control photosynthesis and respiration activity. These mechanisms do obviously not directly influence methane bubble forming.
While other parameters merely had effects on the event size also air pressure indicated a significant influence on event frequency. Since air temperatures and soil temperatures are important for bubble formation, air pressure seems more important on their release (Coulthard et al., 2009; Klapstein et al., 2014; Yu et al., 2014) due to a faster response than heat conduction would allow. Lower air pressure (in case of this study: < 1008 hPa) induces a higher gradient between soil and air. Thereby, gas and bubbles emit more easily (Figure 22), particularly at minimum change points. Very weak events were not influenced by air pressure changes, as Yu et al. (2014) reported as well. Klapstein et al. (2014) explained 57 % of the daily event variations with air pressure changes and depth to seasonal ice. Since in this study almost every situation showed either dropping or rising air pressures (Figure 22), around 60 % of ebullition events showed an air pressure change of at least 0.1 hPa during the previous 30 minutes. Hence, contrary to Tokida et al. (2005) at *Spagnum*-sites also an increase in air pressures could have triggered events.
With exception of methane concentrations no influence of a solely parameter could be determined in this work.

Long-term measurements

The detection of ebullition events with chamber measurements were usually performed in time ranges between two and three minutes. That is enough for a concrete slope between initial and final gas concentration. However, the most important disadvantage of this method is the missing of events instead of a continuous sampling and as such always an incomplete picture of a temporal emission window is observed. Missed events can be compensated with sufficiently and random sampling over diurnal courses as performed in this thesis. Additionally, longer measuring periods about one hour should help to detect more analysable ebullition events as well as possible emission patterns. During the long-term experiments a heating of the chamber inside in warm and sunny weather conditions could be recognised.

Gas saturation effects also appeared in some cases.
Normal measurements showed events in 20 % of all observations (130 events out of 658 measurements), while long-term measurements had events in 61 % of all observations (18 events out of 29 measurements). Regarding the longer time period and partitioning them to normal measurement time scale long-term measurements had with 4 % events of all observations much less events per measurement than in normal measuring periods (Table 6). Thus, saturation and heating may affect longer closed chamber interiors and showed an influence of the experiment to nature. Contrary to this, event properties like event length and event fraction on total flux did not change. That means, a possible flux shift from ebullition to diffusion or plant-mediated transport during long-term measurements is unlikely. Significant influences of environmental parameters could not be found. Nevertheless, with normal two minute measurements a higher event frequency could occur due to a disturbance and trigger by closing the chamber. In that case, the lower event frequency of long-term measurements would be closer to the real fluxes.
Since long-term measurements were not constantly done in the second half of July merely little data from this time period is available and no analysable events occurred in this time. Event frequency increased from June to July and still had a similar development to normal measurements, although much less amounts in July appeared. However, event fractions decreased from June to July and are possibly explainable with temperature effects in the colder June and therefore observations without darkening foil were used. Additionally, total fluxes increased continually, even though it happened with higher amounts in June and August, but lower amounts in July and in total over the summery measuring period. Ebullition proportions showed an exactly contrary development in normal measurements. With long-term measurements in June most ebullition appeared and July as well as August had far less activity. Due to very different results of long-term measurements with lower relative event frequency compared to normal measurements and problems with the analyser from late July on, that could have led to more noise over a longer time period, the long-term experiment series has to be considered as less important nor comparable to normal measurements. Nevertheless, the amounts of long-term measurements in June were very similar to normal measurements and show that long-term observations may help reliably to find more events. If temperature and saturation influences can be avoided either with half a shorter observation period (Pihlatie et al., 2013 recognised non-linearity of fluxes in static chambers over 35 min), with ice packs or air conditioning (Müller et al., 2009) instead of the darkening foil in warm conditions above approximately 20°C, possibly increased diffusion or disabled plant activity will be excluded within the flux measurements.

5 Conclusion

Since a large need exits to understand the role of methane as a greenhouse gas and its process involvement in climate change, the transition from soil into the atmosphere in Arctic permafrost soils has to be determined clearly.
Therefore, an important issue is to improve measurement systems. Under laboratory conditions especially tube heights influenced the flux and a vertically integrating gas sampling turned out to stabilise fluxes, combined with running fans in general. Wind speed measurements showed a better distribution of air with plants in the chamber if fans were angled 90° to a wall. Regarding chamber setups and configurations of the field study only little variations occurred. While inlet tube positions for gas circulation only became important with other settings, especially fans influenced the flux significantly. Worst configurations were flux measurements without running fans particularly for CO_2 due to its high dependence on photosynthesis and plant respiration. Inducing artificial pressure to the soil with fans facing to soil surface has proven another inadequate configuration. Natural fluxes cannot be defined, however, stable fluxes and enhanced natural conditions are possible as shown by the fan configuration of three vertical fans in one corner and an angle parallel to one chamber side wall. Therewith, a horizontal, circulating air stream can be created, which avoids an artificial positive pressure with vertical circulation. Still CO_2 as well as CH_4 were highly dependent on atmospheric conditions with every setup. In conclusion, fans for a better air mixing inside the chamber are necessary for a stable flux.
Ebullition events as one of the emission pathways for CH_4 into the atmosphere had been quantified in different aspects, e.g. ebullition fraction (18 - 28 %) of methane fluxes and ebullition frequency (7 - 42 %) over the summer season. As Windsor et al. (1992) already reported, with higher flux rates more events appeared. In their study of northern Quebec they had a maximal probability of 3.8 % to obtain an event. In this study of north-east Siberia no spring ebullition activity due to snow melt could be clearly recognised. Considering the development of increasing event frequencies the same observations have been made, but correlate with simultaneously temperature rises of atmosphere and soils and hence, more methane productions due to enhanced methanogenesis, as evident in higher total fluxes. Also the length of single events correlated with size and fraction, thus, strongest bubbles last longest and also were slightly influenced by soil wetness. However, flooded measurement sites had significantly more ebullition events and methane fluxes in general. But also the weather situation with air pressure and temperature, as well as the soil conditions with active layer depth, soil temperatures and the vegetation influenced ebullition activity. The proportion of ebullition on the total flux was determined in dependence on these influencing factors during the summer season from 2 to 7 % at mainly flooded sites, with highest activity

around July and August. Due to a relatively long, strong and coincident release of bubbles the observed ebullition may be classified as episodic events, that form in deeper soil layers of just thawed permafrost. The observed event proportions of 0 - 73 % by Yu et al. (2014) and 17 - 52 % by Christensen et al. (2003) fit rather to event fractions in this work, whereas these authors experimented with steady gas fluxes for continuous measuring, *Sphagnum*-peat without plant-mediated transport nor considering of season caused variations. Finally, the transport of methane via ebullition has less proportions on the total flux than plant-mediated transport in the studied area with its aerenchyma plants. Nevertheless, in flooded peatlands with deeply thawed soils and low air pressure it may contribute up to 28 % to the total CH_4-flux.

Further research should consider more constant measuring, investigate interannual development of ebullition, event frequency and improved long-term measurements with a better cooling system at days warmer than 20°C and shorter closing periods to avoid saturation. Besides, more night time measurement seem promising for comparison chamber data with wavelet analyses, since no diurnal cycle nor nightly decreases of ebullition activity could be determined. Additionally plant-mediated transport should be considered for ebullition because of lower event proportions with higher air conducting plant proportion.

Acknowledgements

Especially I like to thank Thomas Foken from University of Bayreuth and Mathias Göckede from the Max-Planck-Institute of Biogeochemistry in Jena for the possibility to realise this Master's thesis and for plentiful advices along the work. Worthy practical and theoretical support I also received from Min Jung Kwon, Carsten Schaller and Fanny Kittler in the field and with scientific work. All the other members of the Max-Planck-Institute for Biogeochemistry in Jena who supported the study in Chersky / Russia are thanked as well. Additionally, I appreciate the help of the Simov family for their intensive logistic and scientific support within the field work and all others who supported me throughout this thesis.

References

Bridgham, S.D., Cadillo-Quiroz, H., Keller, J.K., and Zhuang, Q. (2013). "Methane emissions from wetlands: biogeochemical, microbial, and modeling perspectives from local to global scales". *Global change biology.* 19.5, 1325–1346.

CantyMedia (2014). *Cherskiy, Russia.* URL: `http://www.weatherbase.com/weather/weather.php3?s=32152` (visited on 10/14/2014).

Christensen, T. R., Panikov, N., Mastepanov, M., Joabsson, A., Stewart, A., Öquist, M., Sommerkorn, M., Reynaud, S., and Svensson, B. (2003). "Biotic controls on CO2 and CH4 exchange in wetlands–a closed environment study". *Biogeochemistry.* 64, 337–354.

Christiansen, J.R., Korhonen, J.F.J., Juszczak, R., Giebels, M., and Pihlatie, M. (2011). "Assessing the effects of chamber placement, manual sampling and headspace mixing on CH4 fluxes in a laboratory experiment". *Plant and soil.* 343, 171–185.

Ciais, P., Sabine, C., Bala, G., Bopp, L., Brovkin, V., Canadell, J., Chhabra, A., DeFries, R., Galloway, J., Heimann, M., Jones, C., Le Quéré, C., Myneni, R.B., S., Piao, and Thornton, P. (2013). "Carbon and other biogeochemical cycles". *Climate Change 2013: The Physical Science Basis. Contribution of Working Group I to the Fifth Assessment Report of the Intergovernmental Panel on Climate Change [Stocker, T.F., D. Qin, G.-K. Plattner, M. Tignor, S.K. Allen, J. Boschung, A. Nauels, Y. Xia, V. Bex and P.M. Midgley (eds.)]. Cambridge University Press, Cambridge, United Kingdom and New York, NY, USA.*, 465–570.

Conrad, R. (1996). "Soil microorganisms as controllers of atmospheric trace gases (H2, CO, CH4, OCS, N2O, and NO)." *Microbiological reviews.* 60, 609–640.

Coulthard, T.J., Baird, A.J., Ramirez, J., and Waddington, J.M. (2009). "Methane dynamics in peat: Importance of shallow peats and a novel reduced-complexity approach for modeling ebullition". *Carbon Cycling in Northern Peatlands.* 184, 173–185.

Couwenberg, J. (2009). "Methane emissions from peat soils (organic soils, histosols): facts, MRV-ability, emission factors." *Wetlands International.* UN-FCCC meetings in Bonn.

Crosson, E.R. (2008). "A cavity ring-down analyzer for measuring atmospheric levels of methane, carbon dioxide, and water vapor". *Applied Physics B.* 92, 403–408.

Davidson, E.A., Savage, K.V.L.V., Verchot, L.V., and Navarro, R. (2002). "Minimizing artifacts and biases in chamber-based measurements of soil respiration". *Agricultural and Forest Meteorology.* 113, 21–37.

Drösler, M. (2005). "Trace gas exchange and climatic relevance of bog ecosystems, Southern Germany". PhD thesis. Technische Universität München.

Drösler, M. (2009). "Was haben Moore mit dem Klima zu tun?" *Laufener Spezialbeiträge.* 2, 60–70.

Foken, T. and Wichura, B. (1996). "Tools for quality assessment of surface-based flux measurements". *Agricultural and Forest Meteorology.* 78, 83–105.

Friborg, T., Christensen, T.R., and Søgaard, H. (1997). "Rapid response of greenhouse gas emission to early spring thaw in a subarctic mire as shown by micrometeorological techniques". *Geophysical Research Letters* 24, 3061–3064.

Fritz, C., Pancotto, V.A., Elzenga, J., Visser, E.J.W., Grootjans, A.P., Pol, A., Iturraspe, R., Roelofs, J.G.M., and Smolders, A.J.P. (2011). "Zero methane emission bogs: extreme rhizosphere oxygenation by cushion plants in Patagonia". *New Phytologist.* 190, 398–408.

Gedney, N., Cox, P.M., and Huntingford, C. (2004). "Climate feedback from wetland methane emissions". *Geophysical Research Letters.* 31.20.

Glaser, P.H., Chanton, J.P., Morin, P., Rosenberry, D.O., Siegel, D.I., Ruud, O., Chasar, L.I., and Reeve, A.S. (2004). "Surface deformations as indicators of deep ebullition fluxes in a large northern peatland". *Global Biogeochemical Cycles.* 18, GB1003.

Goodrich, J.P., Varner, R.K., Frolking, S., Duncan, B.N., and Crill, P.M. (2011). "High-frequency measurements of methane ebullition over a growing season at a temperate peatland site". *Geophysical Research Letters.* 38.7, L07404.

Hartmann, D.L., Klein Tank, A.M.G., Rusicucci, M., Alexander, L.V., Broenniman, B., Charabi, Y., Dentener, F.J., Dlugokencky, E.J., Easterling, D.R., Kaplan, A., Soden, B.J., Thorne, P.W., Wild, M., and Zhal, P.M. (2013). "Observations: Atmosphere and surface". *Climate Change 2013: The Physical Science Basis. Contribution of Working Group I to the Fifth Assessment Report of the Intergovernmental Panel on Climate Change [Stocker, T.F., D. Qin, G.-K. Plattner, M. Tignor, S.K. Allen, J. Boschung, A. Nauels, Y. Xia, V. Bex and P.M. Midgley (eds.)]. Cambridge University Press, Cambridge, United Kingdom and New York, NY, USA.*, 159–254.

Hutchinson, G.L. and Rochette, P. (2003). "Non-flow-through steady-state chambers for measuring soil respiration". *Soil Science Society of America Journal.* 67, 166–180.

IPCC, 2013 (2013). "Annex III: Glossary". *Climate Change 2013: The Physical Science Basis. Contribution of Working Group I to the Fifth Assessment Report of the Intergovernmental Panel on Climate Change [Stocker, T.F., D. Qin, G.-K. Plattner, M. Tignor, S.K. Allen, J. Boschung, A. Nauels, Y. Xia, V. Bex and P.M. Midgley (eds.)]. Cambridge University Press, Cambridge, United Kingdom and New York, NY, USA.*, 465–570.

Iturraspe, R. (2010). "Las turberas de Tierra del Fuego y el cambio climático global". *Wetlands International.* Fundación para la Conservación y el Uso Sustentable de los Humedales/ Oficina Argentina de Wetlands International-LAC. Buenos Aires, Argentina.

Joosten, H. and Couwenberg, J. (2009). "Are emission reductions from peatlands MRV-able?" *Wetlands International.* UN-FCCC meetings in Bonn. Germany.

King, J.Y., Reeburgh, W.S., Thieler, K.K., Kling, G.W., Loya, W.M., Johnson, L.C., and Nadelhoffer, K.J. (2002). "Pulse-labeling studies of carbon cycling in Arctic tundra ecosystems: The contribution of photosynthates to methane emission". *Global Biogeochemical Cycles.* 16.4, 10–1.

Klapstein, S.J., Turetsky, M.R., McGuire, A. D., Harden, J.W., Czimczik, C.I., Xu, X., Chanton, J.P., and Waddington, J.M. (2014). "Controls on methane released through ebullition in peatlands affected by permafrost degradation". *Journal of Geophysical Research: Biogeosciences.* 119, 418–431.

Kutzbach, L., Wagner, D., and Pfeiffer, E.-M. (2004). "Effect of microrelief and vegetation on methane emission from wet polygonal tundra, Lena Delta, Northern Siberia". *Biogeochemistry.* 69, 341–362.

Kwon, M.J. (2015). "The impact of small-scale heterogeneity on ecosystem functionality and carbon cycle exchange processes along hydrological gradients in the Siberian Arctic". PhD thesis [in progress]. International Max Planck Research School for Global Biogeochemical Cycles.

Kwon, M.J., Goeckede, M., Wildner, M., Heimann, M., Zimov, N., and Zimov, S. (2014). "Impact of hydrology and vegetation community structure on CO2 and CH4 flux patterns in a permafrost ecosystem in Northeast Siberia". *AGU Fall Meeting December 15-19, 2014.*

Lawrence, B.A., Fahey, T.J., and Zedler, J.B. (2013). "Root dynamics of Carex stricta-dominated tussock meadows". *Plant and soil.* 364, 325–339.

Livingston, G.P. and Hutchinson, G.L. (1995). *Enclosure-based measurement of trace gas exchange: applications and sources of error.* Biogenic trace gases. Oxford. UK: Blackwell Science Cambridge, 14–51.

Martens, C.S., Kelley, C.A., Chanton, J.P., and Showers, W.J. (1992). "Carbon and hydrogen isotopic characterization of methane from wetlands and lakes of the Yukon-Kuskokwim delta, western Alaska". *Journal of Geophysical Research: Atmospheres (1984–2012).* 97, 16689–16701.

McGuire, A.D., Anderson, L.G., Christensen, T.R., Dallimore, S., Guo, L., Hayes, D.J., Heimann, M., Lorenson, T.D., Macdonald, R.W., and Roulet, N. (2009). "Sensitivity of the carbon cycle in the Arctic to climate change". *Ecological Monographs.* 79, 523–555.

Megonigal, J.P., Mines, M.E., and Visscher, P.T. (2005). *Linkages to Trace Gases and Aerobic Processes.* Vol. 8. Biogeochemistry, Band 8. Gulf Professional Publishing, 317.

Merbold, L., Kutsch, W. L., Corradi, C., Kolle, O., Rebmann, C., Stoy, P.C., Zimov, S. A., and Schulze, E.-D. (2009). "Artificial drainage and associated carbon fluxes (CO2/CH4) in a tundra ecosystem". *Global Change Biology.* 15, 2599–2614.

Müller, J., Eschenröder, A., and Diepenbrock, W. (2009). "Through-flow chamber CO2/H2O canopy gas exchange system—Construction, microclimate, errors, and measurements in a barley (Hordeum vulgare L.) field". *Agricultural and Forest Meteorology.* 149, 214–229.

Myhre, G., Shindell, D., Bréon, F.M., Collins, W., Fuglestvedt, J., Huang, J., Koch, D., Lamarque, J.F., Lee, D., Mendoza, B., Nakajima, T., Robock, A., Stephens, G., Takemura, T., and Zhang, H. (2013). "Anthropogenic and natural radiative forcing". *Climate Change 2013: The Physical Science Basis. Contribution of Working Group I to the Fifth Assessment Report of the Intergovernmental Panel on Climate Change [Stocker, T.F., D. Qin, G.-K. Plattner, M. Tignor, S.K. Allen, J. Boschung, A. Nauels, Y. Xia, V. Bex and P.M. Midgley (eds.)]. Cambridge University Press, Cambridge, United Kingdom and New York, NY, USA.*, 658–740.

O'Connor, F. M., Boucher, O., Gedney, N., Jones, C.D., Folberth, G.A., Coppell, R., Friedlingstein, P., Collins, W.J., Chappellaz, J., Ridley, J., and Johnson, C.E. (2010). "Possible role of wetlands, permafrost, and methane hydrates in the methane cycle under future climate change: A review". *Reviews of Geophysics.* 48, RG4005.

Parkin, T., Mosier, A., Smith, J., Venterea, R., Johnson, J., Reicosky, D., Doyle, G., McCarty, G., and Baker, J. (2003). "USDA-ARS GRACEnet chamber-based trace gas flux measurement protocol". *USDA-ARS, Washington DC.*

Pavelka, M., Sedlák, P., Acosta, M., Czerný, R., Taufarová, K., and Janouš, D. (2007). "Chamber techniques versus eddy covariance method during nighttime measurements". *Bioclimatology and natural hazards.*

Pérez-Priego, O., Testi, L., Orgaz, F., and Villalobos, F.J. (2010). "A large closed canopy chamber for measuring CO2 and water vapour exchange of whole trees". *Environmental and experimental botany.* 68, 131–138.

Picarro, INC. (2011). *CRDS Analyzer CO2 CH4 H2O Measurements in Air - Model G2301.* Tech. rep. 3105 Patrick Henry Drive, Santa Clara, CA 95054: PICARRO, INC.

Pihlatie, M.K., Christiansen, J. R., Aaltonen, H., Korhonen, J.F.J., Nordbo, A., Rasilo, T., Benanti, G., Giebels, M., Helmy, M., Sheehy, J., Jones, S., Juszczak, R., Klefoth, R., Lobo-doVale, R., Rosa, A.P., Schreiber, R., Serca, D., Vicca, S., Wolf, B., and Pumpanen, J. (2013). "Comparison of static chambers to measure CH4 emissions from soils". *Agricultural and Forest Meteorology.* 171, 124–136.

Pumpanen, J., Kolari, P., Ilvesniemi, H., Minkkinen, K., Vesala, T., Niinistö, S., Lohila, A., Larmola, T., Morero, M., Pihlatie, M., Janssens, I., Yuste, J.C., Grünzweig, J.M., Reth, S., Subke, J.-A., Savage, K., Kutsch, W., Östreng, G., Ziegler, W., Anthoni, P., Lindroth, A., and Hari, P. (2004). "Comparison of

different chamber techniques for measuring soil CO2 efflux". *Agricultural and Forest Meteorology.* 123, 159–176.

Rella, C. (2010). "Accurate greenhouse gas measurements in humid gas streams using the Picarro G1301 carbon dioxide/methane/water vapor gas analyzer". *White paper, Picarro Inc, Sunnyvale, CA, USA.*

Riederer, M., Serafimovich, A., and Foken, T. (2013). "Net ecosystem CO2 exchange measurements by the closed chamber method and the eddy covariance technique and their dependence on atmospheric conditions–a case study". *Atmospheric Measurement Techniques.* 6, 8783–8805.

Rochette, P. and Hutchinson, G.L. (2005). *Measurement of soil respiration in situ: chamber techniques.* Micrometeorology in Agricultural Systems. Madison. USA: American Society of Agronomy, 247–286.

Rochette, P., Gregorich, E.G., and Desjardins, R.L. (1992). "Comparison of static and dynamic closed chambers for measurement of soil respiration under field conditions". *Canadian Journal of Soil Science.* 72, 605–609.

Rosenberry, D.O., Glaser, P.H., Siegel, D.I., and Weeks, E.P. (2003). "Use of hydraulic head to estimate volumetric gas content and ebullition flux in northern peatlands". *Water Resources Research.* 39, SBH 13.

Rosenberry, D.O., Glaser, P.H., and Siegel, D.I. (2006). "The hydrology of northern peatlands as affected by biogenic gas: current developments and research needs". *Hydrological processes.* 20, 3601–3610.

Sachs, T., Giebels, M., Boike, J., and Kutzbach, L. (2010). "Environmental controls on CH4 emission from polygonal tundra on the microsite scale in the Lena river delta, Siberia". *Global Change Biology.* 16.11, 3096–3110.

Schaller, C. (2015). "Analysis of Methane Emissions in a subarctic permafrost region using Wavelet Transformation and Conditional Sampling". MA thesis [in progress]. University of Bayreuth.

Schuur, E.A.G., Bockheim, J., Canadell, J.G., Euskirchen, E., Field, C.B., Goryachkin, S.V., Hagemann, S., Kuhry, P., Lafleur, P.M., Lee, H., Mazhitova, G., Nelson, F.E., Rinke, A., Romanovsky, V.E., Shiklomanov, N., Tarnocai, C., Venevsky, S., Vogel, J.G., and Zimov, S. (2008). "Vulnerability of permafrost carbon to climate change: Implications for the global carbon cycle". *BioScience.* 58, 701–714.

Smith, S.L., Romanovsky, V.E., Lewkowicz, A.G., Burn, C.R., Allard, M., Clow, G.D., Yoshikawa, K., and Throop, J. (2010). "Thermal state of permafrost in North America: a contribution to the international polar year". *Permafrost and Periglacial Processes.* 21, 117–135.

Tokida, T., Miyazaki, T., and Mizoguchi, M. (2005). "Ebullition of methane from peat with falling atmospheric pressure". *Geophysical Research Letters.* 32, L13823.

Vaughan, D.G., Comiso, J.C., Allison, I., Carrasco, J., Kaser, G., Kwok, R., Mote, P., Murray, T., Paul, F., Ren, J., Rignot, E., Solominam, O., Steffen, K., and Zhang, T. (2013). "Observations: Cryosphere". *Climate Change 2013: The Physical Science Basis. Contribution of Working Group I to the Fifth Assessment Report of the Intergovernmental Panel on Climate Change [Stocker, T.F., D. Qin, G.-K. Plattner, M. Tignor, S.K. Allen, J. Boschung, A. Nauels, Y. Xia, V. Bex and P.M. Midgley (eds.)]. Cambridge University Press, Cambridge, United Kingdom and New York, NY, USA.*, 317–382.

Werle, P. and Kormann, R. (2001). "Fast chemical sensor for eddy-correlation measurements of methane emissions from rice paddy fields". *Applied Optics.* 40, 846–858.

Whalen, S.C. (2005). "Biogeochemistry of methane exchange between natural wetlands and the atmosphere". *Environmental Engineering Science.* 22, 73–94.

Windsor, J., Moore, T.R., and Roulet, N.T (1992). "Episodic fluxes of methane from subarctic fens". *Canadian Journal of Soil Science.* 72, 441–452.

Xu, L., Furtaw, M.D., Madsen, R.A., Garcia, R.L., Anderson, D.J., and McDermitt, D.K. (2006). "On maintaining pressure equilibrium between a soil CO2 flux chamber and the ambient air". *Journal of Geophysical Research: Atmospheres (1984–2012).* 111, D08S10.

Yu, Z., Slater, L.D., Schäfer, K.V.R., Reeve, A.S., and Varner, R.K. (2014). "Dynamics of methane ebullition from a peat monolith revealed from a dynamic flux chamber system". *Journal of Geophysical Research: Biogeosciences.* 119, 1789–1806.

Zhang, T., Barry, R.G., Knowles, K., Heginbottom, J.A., and Brown, J. (1999). "Statistics and characteristics of permafrost and ground-ice distribution in the Northern Hemisphere 1". *Polar Geography.* 23, 132–154.

Zimov, S.A. (2005). "Pleistocene park: return of the mammoth's ecosystem". *Science.* 308, 796–798.

Zimov, S.A., Voropaev, Y.V., Semiletov, I.P., Davidov, S.P., Prosiannikov, S.F., Chapin, F. SIII, Chapin, M.C., Trumbore, S., and Tyler, S. (1997). "North Siberian lakes: a methane source fueled by Pleistocene carbon". *Science.* 277, 800–802.

Zimov, S.A., Schuur, E.A.G., and Chapin III, F. S. (2006). "Permafrost and the global carbon budget". *Science (Washington).* 312, 1612–1613.

Appendix

Figure A-1: Cotton grass on partly still frozen permafrost soil.

Figure A-2: Vegetation at field site in first half of June with flooding, tussocks, willow shrubs (left) and in July with less flooding, tussocks, cotton grass, willow shrubs and larches in far background (right).

Table A-3: Means of all test configurations with each at least three repetitions measured from April 28th to May 23rd 2014 under laboratory conditions. Diurnal measurements are excluded.

Set No.	Inlet tube position [cm]	Inlet tube height [cm]	Fan No. used	Fan angle [°] from chamber wall	Plant
1	horizontal (left to right corner)	5	1+2+3	45	-
	horizontal (left to right corner)	15	1+2+3	45	-
	horizontal (left to right corner)	30	1+2+3	45	-
	horizontal (left to right corner)	45	1+2+3	45	-
	horizontal (left to right corner)	55	1+2+3	45	-
	horizontal (left to right corner)	5	-	-	-
	horizontal (left to right corner)	15	-	-	-
	horizontal (left to right corner)	30	-	-	-
	horizontal (left to right corner)	45	-	-	-
	horizontal (left to right corner)	55	-	-	-
2	diagonal 10 (left to right corner)	10+30+50	1+2+3	45	-
	diagonal 40 (left to right corner)	10+30+50	1+2+3	45	-
	diagonal 55 (left to right corner)	10+30+50	1+2+3	45	-
	diagonal 70 (left to right corner)	10+30+50	1+2+3	45	-
	diagonal 10 (left to right corner)	10+30+50	-	-	-
	diagonal 25 (left to right corner)	10+30+50	-	-	-
	diagonal 40 (left to right corner)	10+30+50	-	-	-
	diagonal 55 (left to right corner)	10+30+50	-	-	-
	diagonal 70 (left to right corner)	10+30+50	-	-	-
3	diagonal 40 (chamber centre)	10+30+50	1	45	-
	diagonal 40 (chamber centre)	10+30+50	2	45	-
	diagonal 40 (chamber centre)	10+30+50	3	45	-
	diagonal 40 (chamber centre)	10+30+50	1+2	45	-
	diagonal 40 (chamber centre)	10+30+50	1+3	45	-
	diagonal 40 (chamber centre)	10+30+50	2+3	45	-
4	diagonal 40 (chamber centre)	10+30+50	1+2+3	0	-
	diagonal 40 (chamber centre)	10+30+50	1+2+3	22.5	-
	diagonal 40 (chamber centre)	10+30+50	1+2+3	45	-
	diagonal 40 (chamber centre)	10+30+50	1+2+3	67.5	-
	diagonal 40 (chamber centre)	10+30+50	1+2+3	90	-
5	vertical (20+40), front side	20+40	1+2	45	yes
	vertical (20+40), left corner	20+40	1+2	45	yes
	vertical (20+40), right corner	20+40	1+2	45	yes
6	vertical (10+30+50), front side	10+30+50	1+2+3	45	yes
	vertical (10+30+50), front side	10+30+50	1+2+3	90	yes
	vertical (10+30+50), left corner	10+30+50	1+2+3	45	yes
	vertical (10+30+50), left corner	10+30+50	1+2+3	90	yes
	vertical (10+30+50), opposite corner	10+30+50	1+2+3	45	yes
	vertical (10+30+50), opposite corner	10+30+50	1+2+3	90	yes
	vertical (10+30+50), right corner	10+30+50	1+2+3	45	yes
	vertical (10+30+50), right corner	10+30+50	1+2+3	90	yes

continued on next page

Set No.	Inlet tube position [cm]	Inlet tube height [cm]	Fan No. used	Fan angle [°] from chamber wall	Plant
7	vertical (10), front side	10	1+2+3	45	yes
	vertical (10), front side	10	-	-	yes
	vertical (10), front side	10	1+2+3	90	yes
	vertical (10), right corner	10	1+2+3	45	yes
	vertical (10), right corner	10	-	-	yes
	vertical (10), right corner	10	1+2+3	90	yes
	vertical (30), front side	30	1+2+3	45	yes
	vertical (30), front side	30	-	-	yes
	vertical (30), front side	30	1+2+3	90	yes
	vertical (30), right corner	30	1+2+3	45	yes
	vertical (30), right corner	30	-	-	yes
	vertical (30), right corner	30	1+2+3	90	yes
	vertical (50), front side	50	1+2+3	45	yes
	vertical (50), front side	50	-	-	yes
	vertical (50), front side	50	1+2+3	90	yes
	vertical (50), right corner	50	-	-	yes
	vertical (50), right corner	50	1+2+3	90	yes

Table A-4: Mean wind speeds [m s^{-1}] measured with 1 Hz and five times per value for five different sets of plants and fan configurations (see Table 3). Visualisation of sets is shown in Figure 7.

Height	Set	1. empty, fans 45°	2. with obstacle, fans 45°	3. with plant, fans 45°	4. with plant, fans 90°	5. with plant, fans 0°, 90°
45 cm	left corner	0.32	0.26	0.20	0.45	0.12
	right corner	0.32	0.19	0.29	0.47	0.19
	opposite	0.40	0.22	0.11	0.59	0.19
	behind	-	0.26	0.64	0.70	0.63
	in front	0.63	0.58	0.58	0.46	-
	centre	0.39	0.36	0.40	0.37	0.32
	without fans	0.02	0.03	0.02	0.02	0.04
	front side	0.49	0.39	0.52	0.99	0.38
	left side	0.39	0.23	0.19	0.51	0.25
	back side	0.28	0.22	0.21	0.46	0.23
	right side	0.31	0.43	0.60	0.63	0.46
25 cm	left corner	0.34	0.31	0.29	0.78	0.19
	right corner	0.32	0.37	0.17	0.36	0.48
	opposite	0.38	0.27	0.19	0.50	0.18
	behind	-	0.57	0.82	0.60	1.02
	in front	0.67	0.63	0.78	0.71	-
	centre	0.75	0.15	0.05	0.05	0.16
	without fans	0.02	0.02	0.03	0.04	0.02
	front side	0.59	0.56	0.65	0.89	0.50
	left side	0.41	0.27	0.23	0.57	0.19
	back side	0.48	0.26	0.26	0.66	0.29
	right side	0.61	0.45	0.56	0.57	0.37
5 cm	left corner	0.32	0.25	0.54	0.85	0.64
	right corner	0.27	0.30	0.15	0.32	0.34
	opposite	0.40	0.28	0.30	0.35	0.28
	behind	-	0.56	0.89	1.07	0.67
	in front	0.64	0.67	0.63	0.87	-
	centre	0.41	-	-	-	-
	without fans	0.02	0.02	0.02	0.02	0.02
	front side	0.65	1.03	0.65	1.16	1.15
	left side	0.43	0.36	0.45	0.74	0.39
	back side	0.46	0.45	0.34	0.56	0.24
	right side	0.56	0.47	0.83	0.71	0.87

Table A-5: Mean fluxes [mgC m^{-2} min^{-1}] for chamber setup measurements at different setup configurations (↑: high; ↓: low; →: mediate; (): number of data points; $p \leq 0.05$*; $p \leq 0.01$**; $p \leq 0.001$***; red: reference values; grey: : smaller; black: larger; $maximum_M$; $minimum_m$).

Chamber site	Normal (fans 45°)	Fans 90°	No fans	Inlet tubes on ground	Inlet tubes on ground (no fans)	Fans to soil (fans 45°)
1. Single chamber comparison						
a) CH_4						
1/0 (16)	0.028 (3)	0.029 (3) $_M$	0.017 (3)*** $_m$	0.027 (3)	0.029 (2)	0.026 (2)
2/6 (15)	0.097 (3) $_m$	0.099 (3)	0.099 (3)	0.103 (3)	NA	0.114 (3)* $_M$
b) CO_2						
1/0 (16)	-4.901 (3)	-4.625 (3)	-5.956 (3)* $_m$	-4.643 (3)	-3.447 (2)*** $_M$	-4.642 (2)
1/3 (15)	-3.429 (2)	-2.621 (3) $_M$	-4.763 (2)	-4.029 (2)	-8.023 (3)** $_m$	-3.155 (3)
2/4 (12)	-1.675 (3) $_m$	-1.280 (3)	-1.275 (3) $_M$	-1.286 (3)	NA	NA
2/6 (15)	-2.008 (3)	-2.102 (3)	-2.208 (3) $_m$	-1.307 (3)*	NA	-1.100 (3)** $_M$
2. Flooding						
a) wet soil CH_4						
1/0, 2/6 (31)	0.063 (6)	0.064 (6)	0.058 (6)	0.065 (6)	0.029 (2) $_m$	0.079 (5) $_M$
b) wet soil CO_2						
1/0, 2/6 (31)	-3.455 (6)	-3.364 (6)	-4.082 (6) $_m$	-2.975 (6)	-3.447 (2)	-2.527 (5) $_M$
c) dry soil CO_2						
1/3, 2/4 (27)	-2.377 (5)	-1.951 (6) $_M$	-2.670 (5)	-2.383 (5)	-8.023 (5)*** $_m$	-3.155 (3)
3. Atmospheric conditions						
a) air pressure CH_4						
↑ 2/6 (15)	0.097 (3) $_m$	0.099 (3)	0.099 (3)	0.103 (3)	NA	0.114 (3)* $_M$
↓ 1/0 (16)	0.028 (3)	0.029 (3)$_M$	0.017 (3)*** $_m$	0.027 (3)	0.029 (2)	0.026 (2)
b) air pressure CO_2						
↑ 2/4, 2/6 (27)	-1.842 (6) $_m$	-1.691 (6)	-1.741 (6)	-1.296 (6)	NA	-1.100 (3) $_M$
↓ 1/0, 1/3 (31)	-4.312 (5)	-3.623 (6) $_M$	-5.479 (5)	-4.397 (5)	-6.192 (5)* $_m$	-3.750 (5)
c) air temperature CH_4						
↑ 1/0 (16)	0.028 (3)	0.029 (3) $_M$	0.017 (3)*** $_m$	0.027 (3)	0.029 (2)	0.026 (2)
↓ 2/6 (15)	0.097 (3) $_m$	0.099 (3)	0.099 (3)	0.103 (3)	NA	0.114 (3)* $_M$
d) air temperature CO_2						
↑ 1/0, 1/3 (31)	-4.312 (5)	-3.623 (6) $_M$	-5.479 (5)	-4.397 (5)	-6.192 (5)* $_m$	-3.750 (2)
→ 2/4 (12)	-1.675 (3) $_m$	-1.280 (3)	-1.275 (3) $_M$	-1.286 (3)	NA	NA
↓ 2/6 (15)	-2.008 (3)	-2.102 (3)	-2.208 (3) $_m$	-1.307 (3)*	NA	-1.100 (3)** $_M$
4. Gas fluxes						
a) CH_4						
1/0, 2/6 (31)	0.063 (6)	0.064 (6)	0.058 (6)	0.065 (6)	0.029 (2) $_m$	0.079 (5) $_M$
b) CO_2						
1/0, 1/3, 2/4, 2/6 (58)	-2.965 (11)	-2.657 (12) $_M$	-3.440 (11)	-2.706 (11)	-6.192 (5)* $_m$	-2.756 (8)

Table A-6: Ebullition proportion of total flux [%] for every single chamber; dash: no events or no measurements

Chamber	June	July	August	Total	Percentage of cotton grass	Percentage of tussock shaped sedges
1/0	-	$0.2^{(*)}$	3.4	1.1	88.9	0
1/1	-	-	-	-	57.1	42.9
1/2	-	-	$0.9^{(*)}$	$0.3^{(*)}$	15.8	84.2
1/3	-	-	-	-	0	95.7
1/4	-	-	-	-	20	65.0
1/5	-	-	-	-	0	100
1/6	-	-	-	-	0	94.7
1/7	-	-	-	-	0	90.9
1/8	-	-	-	-	0	90.5
1/9	-	-	-	-	0	21.7
B1/3	-	7.3	$2.4^{(*)}$	5.6	-	-
B1/7	-	$2.4^{(*)}$	-	$1.3^{(*)}$	-	-
S1/3	-	-	$3.9^{(*)}$	$1.4^{(*)}$	-	-
S1/7	-	-	-	-	-	-
2/0	-	$0.5^{(*)}$	3.9	2.2	0	84.2
2/1	-	10.5	$7.3^{(*)}$	9.1	100	0
2/2	-	4.4	8.6	5.3	80	0
2/3	$8.3^{(*)}$	23.3	15.8	15.8	16.7	0
2/4	-	-	-	-	0	62.5
2/5	-	-	-	-	0	78.9
2/6	1.8	3.3	4.0	3.2	64.7	0
2/7	-	16.2	4.5	10.9	100	0
2/8	-	9.3	9.1	9.1	91.7	0
2/9	-	28.1	10.6	19.3	100	0

Statutory Declaration / Selbstständigkeitserklärung

This Master's thesis is written on my own independently without any foreign sources or support, beside herein declared. Neither this, nor a similar work, has been published or presented to an examination committee before to obtain an academic degree.

- - - - - - - - -

Die vorgelegte Masterarbeit wurde von mir selbstständig angefertigt. Weder wurden unlautere Mittel verwendet, noch verwendete Quellen verschwiegen oder die Arbeit bereits zur Erlangung eines akademischen Grades eingereicht.

Bayreuth, February 2015